Kanegane H, Taneichi H, Nomura K, Wada T, Yachie A, Imai K, Ariga T, et al.	Successful bone marrow transplantation with reduced intensity conditioning in a patient with delayed-onset adenosine deaminase deficiency.	Pediatr Transplant.	17	E29-E32	2013
Horino S, Sasahara YI, Ariga T et al.	Selective expansion of regulatory T cells in mixed chimera after allogeneic bome marrow transplantation in a patient with IPEX syndrome.	Pediatr Transplant.	18	E25-E30	2014
Konomoto T, Tanaka E, Imamura H, Orita M, Sawada H, Nunoi H.	Nephrotic syndrome complicated by idiopathic central diabetes insipidus.	Pediatr Nephrol			in press
Yamada A, Moritake H, Shimonodan H, Yokogami K, Takeshima H, Marutsuka K, Nunoi H.	Efficacy of temozolomide in a central nervous system relapse of neuroblastoma with O 6 -methylguanine methyltransferase (MGMT) promoter methylation.	J Pediatr Hematol Oncol	35	E38-41	2013
布井博幸	過剰炎症と免疫療法	小児科診療	76	467-475	2013
Nemoto A, Inukai T, Uno K, Kiyokawa N, Miyagawa Y, Takahashi K, Sato H, … Fujimoto J, Inaba T, Sugita K.	Diverse underlying proliferation response to growth factors in imatinib-treated Philadelphia chromosome-positive leukemias.	Leukemia Res.	37	93-101	2013
Ueno H, Okita H, Akimoto S, Kobayashi K, Nakabayashi K, Hata K, Fujimoto J, Hata J, Fukuzawa M, Kiyokawa N.	DNA methylation profile distinguishes clear cell sarcoma of the kidney from other pediatric renal tumors.	PLoS One.	8	e62233	2013
Kiyokawa N, Iijima A, Tomita O, Miharu M, Hasegawa D, Kobayashi K, … Fujimoto J, et al.	Significance of CD66c expression in childhood acute lymphoblastic leukemia.	Leukemia Res.			in press
Enosawa S; Horikawa R; Yamamoto A, Sakamoto S, Shigeta T, Nosaka S, Fujimoto J, Tanoue A, Nakamura K, Umezawa A, Matsubara Y, Matsui A and Kasahara M.	Hepatocyte transplantation using the living donor reduced-graft in a baby with ornithine transcarbamylase deficiency: a novel source for hepatocytes.	Liver Transplant.			in press

書　籍

著者氏名	論文タイトル	書籍全体の編集者名	書　籍　名	出版社名	出版地	出版年	ページ
布井博幸	インフルエンザの重症化因子	高病原性鳥インフルエンザの診断・治療に関する国際連携研究班	重症新型インフルエンザ診断と治療の手引き	メディカル・サイエンス・インターナショナル	東京	2013	14-17, 125-130
唐沢直希、中原彰彦、布井博幸	第14章　小児の発熱治療　禁忌事項	原寿郎	小児の発熱とAtoZ	診断と治療社	東京	2012	248-250
布井博幸	慢性肉芽腫症の病態解析	鈴木和男	血管炎　増刊号	日本臨床社	大阪	2013	601-604
布井博幸、西村豊樹、中原彰彦	インフルエンザ感染における重症合併症（インフルエンザ脳症）	水澤英洋	神経感染症（第２版）	日本臨床社	大阪	2013	652-656
布井博幸	Jordans 異常	田村和夫	血液症候群（第２版）	日本臨床社	大阪	2013	101-104

VI.　研究成果の印刷物・別刷

Clinical Immunology (2013) 147, 122–128

available at www.sciencedirect.com

Clinical Immunology

www.elsevier.com/locate/yclim

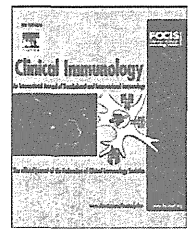

Thalidomide attenuates excessive inflammation without interrupting lipopolysaccharide-driven inflammatory cytokine production in chronic granulomatous disease☆

Toshinao Kawai [a,b,*], Nobuyuki Watanabe [a], Midori Yokoyama [a], Katsuhiro Arai [c], Shinji Oana [d], Shizuko Harayama [a,e], Kozo Yasui [f], Tsutomu Oh-ishi [g], Masafumi Onodera [a,b]

[a] *Department of Human Genetics, National Center for Child Health and Development, Tokyo, Japan*
[b] *Division of Immunology, National Center for Child Health and Development, Tokyo, Japan*
[c] *Division of Gastroenterology and Hepatology, National Center for Child Health and Development, Tokyo, Japan*
[d] *Department of Interdisciplinary Medicine, National Center for Child Health and Development, Tokyo, Japan*
[e] *Department of Pediatrics, The Jikei University School of Medicine, Tokyo, Japan*
[f] *Department of Pediatrics, Hiroshima City-Hospital, Hiroshima, Japan*
[g] *Division of Infectious Diseases, Immunology and Allergy, Saitama Children's Medical Center, Saitama, Japan*

Received 23 August 2012; accepted with revision 7 March 2013

KEYWORDS
Chronic granulomatous disease;
Cytokine;
Thalidomide;
Inflammatory bowel disease;
Reactive oxygen species

Abstract Chronic granulomatous disease (CGD) is a rare inherited disorder characterized by an inability to produce reactive oxygen species, resulting in recurrent life-threatening infections. Curiously, half of the patients with CGD suffer from aseptic bowel inflammation (CGD colitis) due to dysregulated inflammation induced by TNF-α and IL-1β. Thus, developing therapies that regulate excessive inflammatory responses without interrupting antimicrobial immunity would benefit CGD colitis patients. Here, we show that thalidomide suppressed TNF-α-induced NF-κB activation and ATP-induced IL-1β secretion, but did not interrupt the production of IL-1β, IL-6, IL-8, and TNF-α in response to lipopolysaccharide in CGD monocytes. We report on a CGD colitis patient that showed decreased bowel inflammation characterized by reduced serum levels of inflammatory cytokines without evidence of progression of fungal and bacterial infections present at initiation of thalidomide therapy. Our results suggest that thalidomide could be an efficacious therapeutic option for patients with CGD colitis suffering from serious infections.

☆ Thalidomide regulates TNF-α-induced NF-κB activation, but does not interrupt lipopolysaccharide-driven inflammatory cytokine production in monocytes isolated from patients with chronic granulomatous disease.

* Corresponding author at: Department of Human Genetics, National Center for Child Health and Development, 2-10-1 Okura, Setagaya-ku, Tokyo, 157-8535, Japan. Fax: +81 3 5494 7035.
E-mail address: kawai-t@ncchd.go.jp (T. Kawai).

1521-6616/$ - see front matter © 2013 Elsevier Inc. All rights reserved.
http://dx.doi.org/10.1016/j.clim.2013.03.004

1. Introduction

Reactive oxygen species (ROS) generated by cellular nicotinamide adenine dinucleotide phosphate (NADPH) oxidase play an important role in killing microorganisms ingested by phagocytes. In addition, ROS function as pleiotropic signals in various inflammatory contexts. For example, ROS activate nuclear factor-κB (NF-κB), which produces inflammatory cytokines and facilitates formation of the inflammasome consisting of Nod-like receptor family, pyrin domain containing 3 (NLRP3), ASC, cardinal, and pro-caspase-1, which cleaves into caspase-1 and converts pro-interleukin-1β (IL-1β) to IL-1β [1,2]. Chronic granulomatous disease (CGD) is a primary immunodeficiency resulting from the inability to produce ROS due to defects in NADPH oxidase activity [3]. CGD patients suffer from recurrent infection and frequently develop CGD-associated bowel inflammation (CGD colitis) in the absence of any demonstrable infection [4]. The underlying mechanism of CGD colitis is not fully understood; however, dysregulated inflammatory cytokine production, such as IL-1β and tumor necrosis factor-α (TNF-α), by monocytes and macrophages is thought to contribute to the disease [1,5]. This concept is supported by many clinical reports that neutralizing anti-TNF-α or immunosuppressive drugs, such as steroids or azathioprine, effectively mitigate CGD colitis clinical symptoms. Notably, the use of these drugs results in an increased susceptibility to severe infections [4,5].

Thalidomide, originally developed in the 1950s as a tranquilizer, was discontinued when its potent teratogenic effects resulted in catastrophic birth defects in the 1960s. It is recently being reconsidered for its unique and pleiotropic medical effects, such as immunomodulation and anti-inflammatory properties. Thalidomide potentially reduces inflammation by blocking nuclear localization of NF-κB and inhibiting inflammatory cytokine production in patients with chronic inflammatory diseases such as Behcet's disease, rheumatoid arthritis, and Crohn disease [4,6–8]. So far, there are case reports regarding three patients with CGD colitis who were treated with thalidomide [4,9], although the immunomodulatory effect of thalidomide on CGD monocytes has not been described. In this report we show that thalidomide suppressed TNF-α-induced NF-κB activation and adenosine triphosphate (ATP)-induced IL-1β secretion while not interrupting lipopolysaccharide (LPS)-driven inflammatory cytokine production in CGD monocytes. We also show that thalidomide treatment improved bowel inflammation by reducing serum TNF-α levels without increasing susceptibility to infection in a CGD colitis patient.

2. Materials and methods

2.1. Monocyte isolation and stimulation

All experiments were performed following receipt of informed consent from patients with X-linked CGD or their parents as part of a protocol approved by the Institutional Review Board of the National Center for Child Health and Development. Monocytes isolated from peripheral blood by an antibody-mediated cell enrichment procedure from RossettSep (StemCell Technologies, Canada) were stimulated with serial concentrations of LPS and with carbonyl cyanide 3-chlorophenylhydrazone (CCCP) (Sigma-Aldrich, St. Louis, MO) or thalidomide (Fujimoto Pharmaceutical Corporation, Japan).

2.2. Caspase-1 activation and cytokine production

Caspase-1 activity was assessed by flow cytometry on a FACSAria IIIu (Becton Dickinson Biosciences, San Diego, CA) using caspase-1 FLICA (Immunochemistry Technologies, Bloomington, MN), a fluorescent inhibitor of active caspase-1, according to the manufacturer's instructions [1]. Human IL-1β, IL-6, IL-8, and TNF-α levels were determined in 5×10^6 cells/ml monocyte cell cultures by quantitative multiplex detection using Milliplex (Millipore, Billerica, MA).

2.3. NF-κB activation

Nuclear extracts were prepared using NE-PER nuclear and cytoplasmic extraction kits (Thermo Scientific, Rockford, IL), and were used to assess NF-κB activation using a transcription factor kit for NF-κB (Thermo Scientific) according to the manufacturer's instructions. Experiments were done in duplicate.

2.4. IL-1β production

Monocytes were primed with 100 ng/ml LPS alone or LPS plus serial concentrations of thalidomide for 2 h before addition of 5 mM ATP. IL-1β levels in monocyte supernatants were measured by quantitative multiplex detection using Milliplex [10].

2.5. Immunologic assessment of a CGD patient treated with thalidomide

A three-year-old boy developed CGD colitis at age 11 months during treatment with isoniazid for *Bacille Calmette–Guérin* (*BCG*)-related lymphadenitis. Despite several trials with anti-inflammatory drugs, the patient suffered from persistent bowel inflammation and developed pulmonary aspergillosis 3 weeks prior to thalidomide therapy. After informed consent was received from his parents, he was treated with daily oral thalidomide for 8 weeks before undergoing conditioning for bone marrow transplantation. Peripheral blood lymphocyte subsets were determined with FACSAria IIIu using anti-human CD3, CD4, CD19, CD31, and CD45RA monoclonal antibodies conjugated with fluorescein isothiocyanate, phycoerythrin (PE), peridinin–chlorophyll proteins-Cy5.5, allophycocyanin, or PE-Cy7 (BioLegend, San Diego, CA).

2.6. Statistics

Experimental data were reported as the mean ± standard deviation (s.d.). Significance was determined by Student's *t*-test. Error bars indicate mean ± s.d.

3. Results

3.1. Thalidomide does not block caspase-1 activation or IL-1β production following LPS stimulation in CGD monocytes

Monocytes are capable of activating caspase-1 to process and release IL-1β by LPS signaling through Toll-like receptor 4 (TLR4) [11]. In keeping with these results [12], LPS induced capase-1 activation and IL-1β production in a dose-dependent manner in CGD monocytes as well as in healthy control monocytes (Figs. 1a–c), suggesting that ROS generated by NADPH oxidase was dispensable for caspase-1 activation and conversion of pro-IL-1β to IL-1β. To assess the effect of thalidomide on caspase-1 activation and IL-1β production, monocytes were cultured with LPS in the presence of thalidomide and the levels of active caspase-1 in monocytes and IL-1β in culture supernatants were measured. Thalidomide did not show any significant effects on caspase-1 activation and IL-1β production in monocytes from healthy control and CGD patients (Figs. 1d–e). On the other hand, CCCP, a chemical inhibitor of ROS-generating mitochondria [13,14], significantly reduced LPS-driven IL-1β production in CGD monocytes and healthy control monocytes (Fig. 1e). Since CCCP showed no effect on caspase-1 activation (Fig. 1d), it was likely that CCCP inhibited IL-1β production in monocytes stimulated with LPS independent of the inflammasome.

3.2. Lipopolysaccharide initiates inflammatory cytokine production in CGD monocytes treated with thalidomide

LPS signaling via TLR4 induces the production of IL-6, IL-8, and TNF-α, which is required for resistance against pathogenic microorganisms. Whereas maturation of IL-1β depends on inflammasome oligomerization followed by caspase-1 activation, the cytokines are secreted through activation of the NF-κB pathway. CGD monocytes had higher IL-6 and

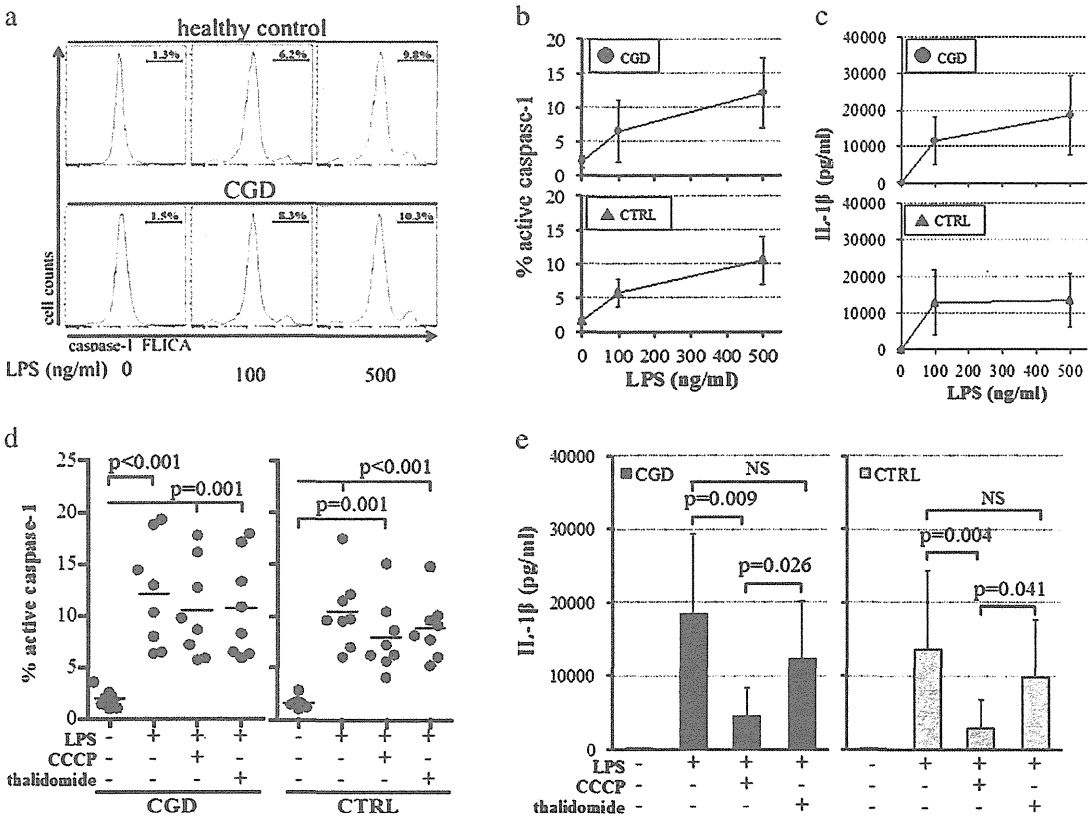

Figure 1 Lipopolysaccharide activates caspase-1 and induces IL-1β secretion in CGD monocytes treated with thalidomide. (a–c) Monocytes were stimulated with 0, 100, and 500 ng/ml lipopolysaccharide (LPS) for 4 h. (a) The numbers above the bracketed lines indicate the percentage of active caspase-1-positive monocytes quantified using FLICA. (b) Active caspase-1 levels were assessed in monocytes from CGD patients (black circles) and healthy controls (CTRL; triangles). (n = 8) (c) LPS-driven IL-1β production was assessed in monocytes from CGD patients (black circles) and healthy controls (triangles). (n = 8) (d) Shown is the percentage of active caspase-1-positive cells in monocytes stimulated with 500 ng/ml LPS alone or LPS plus 50 nM carbonyl cyanide 3-chlorophenylhydrazone (CCCP) or 10 μg/ml thalidomide for 4 h. (e) Secretion levels of IL-1β were assessed in monocytes from CGD patients (black bars) and healthy controls (gray bars) after stimulation with 500 ng/ml LPS alone or LPS plus 50 nM CCCP or 10 μg/ml thalidomide for 4 h. (n = 8) NS, not significant.

TNF-α production in response to LPS than that of healthy controls, suggesting that CGD monocytes retained the ability to activate and easily release more inflammatory cytokines at the time of infection (Fig. 2). Moreover, thalidomide did not impair the production of IL-6, IL-8, and TNF-α in monocytes stimulated with LPS both from healthy controls and CGD patients, while CCCP strongly suppressed the LPS-driven production of cytokines similar to IL-1β (Fig. 2). Since production of inflammatory cytokines depends on NF-κB signaling and is less associated with inflammasome oligomerization induced by mitochondria-generating ROS, CCCP may inhibit cytokine production in a manner not susceptible to ROS inhibitors. Again, thalidomide did not interfere with production of inflammatory cytokines by LPS.

3.3. Thalidomide suppresses NF-κB activation induced by TNF-α

Having identified that thalidomide had no effect on the production of cytokines induced by LPS, we next assessed the effect of thalidomide on the signal cascade induced by TNF signaling. When peripheral blood mononuclear cells (PBMCs) were preincubated with thalidomide and then stimulated with TNF-α, thalidomide significantly suppressed the DNA-binding ability of NF-κB in a dose-dependent manner in monocytes from CGD patients and healthy controls (Fig. 3). These results are identical to those previously described, that is, thalidomide suppressed NF-κB activation induced by TNF-α, but did not inhibit the activation by LPS [15]. This suggests that thalidomide can suppress excessive inflammation induced by TNF-α signals associated with granuloma formation in CGD colitis without interfering with LPS-induced inflammatory cytokine production.

3.4. Thalidomide suppresses the secretion of IL-1β induced by ATP in CGD monocytes

More than 95% of pro-IL-1β in monocytes stimulated by LPS is unprocessed and dispersed throughout the cytoplasm

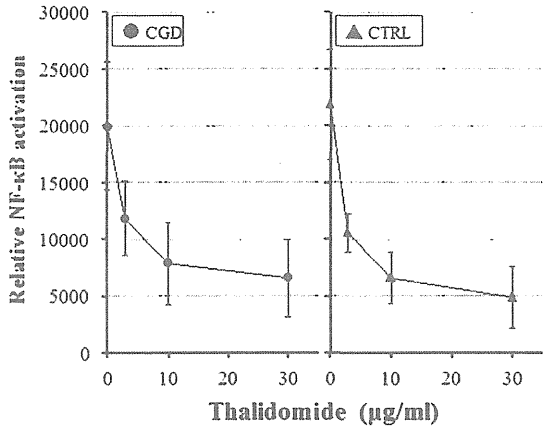

Figure 3 Thalidomide suppresses the TNF-α-mediated DNA-binding ability of NF-κB. Nuclear extracts from peripheral blood mononuclear cells (PBMCs) from CGD patients (circle) and healthy controls (triangle) were assessed for the DNA-binding ability of NF-κB at each indicated concentration of thalidomide. PBMCs were treated with serial concentrations of thalidomide for 2 h and then stimulated with 10 ng/ml TNF-α for 30 min at 37°. NF-κB activation was monitored by luciferase activity. (n = 8).

absent in a secondary stimulus. Recently, the stimulus is thought to be signaling through pannexin-1, which functions as a hemichannel, induced by the binding of ATP to P2X7 receptors [16,17]. Indeed, application of ATP to human monocytes did not induce a large amount of IL-1β secretion; ATP induced significantly higher levels of IL-1β secretion in LPS-primed monocytes from CGD patients and healthy controls (Fig. 4 compared to Fig. 1e). Interestingly, thalidomide decreased IL-1β secretion from CGD monocytes in a dose-dependent manner (Fig. 4). Although the exact mechanism remains unclear, this suggests that thalidomide inhibits IL-1β secretion enhanced by ATP in CGD monocytes.

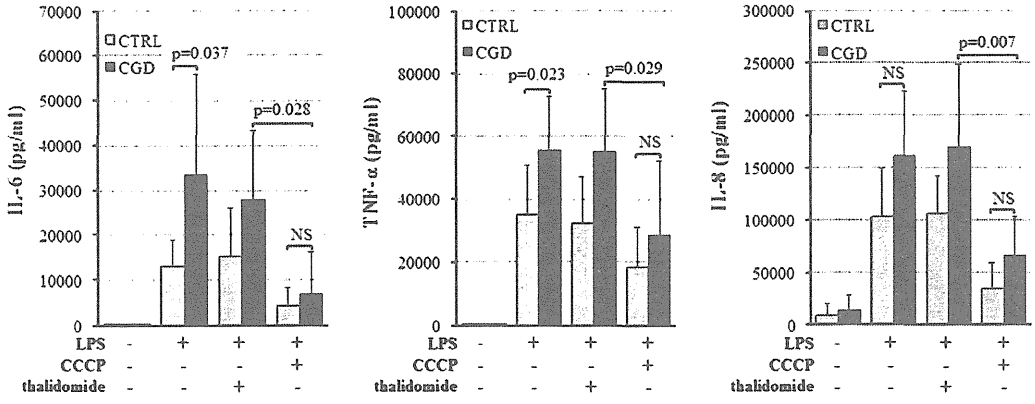

Figure 2 Lipopolysaccharide-driven inflammatory cytokine production was not impaired in CGD monocytes treated with thalidomide. Monocytes were stimulated with 500 ng/ml LPS alone or LPS plus 50 nM carbonyl cyanide 3-chlorophenylhydrazone (CCCP) or 10 μg/ml thalidomide for 4 h. CGD monocytes (black bars) released significantly higher amounts of IL-6 and TNF-α in response to LPS than monocytes from healthy controls (gray bars: CTRL). There was no difference in LPS-driven IL-8 secretion between monocytes from CGD patients and healthy controls (p = 0.053). (n = 8). NS, not significant.

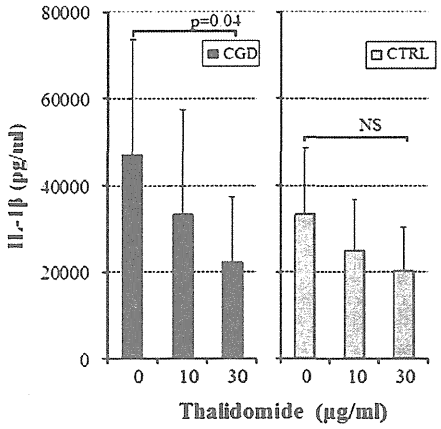

Figure 4 IL-1β secretion induced by ATP in CGD monocytes. After activation by 100 ng/ml LPS alone or LPS plus serial concentrations of thalidomide for 2 h, ATP was added to achieve a final concentration of 5 mM and the samples were incubated at 37° for 4 h. Secretion of IL-1β into culture supernatants was determined in 5 × 10^6 cells/ml monocyte cell cultures from CGD patients (black bars) and healthy controls (gray bars: CTRL). (n = 8) NS, not significant.

3.5. Thalidomide therapy improves clinical symptoms of CGD colitis without impairing control of *Aspergillus* pneumonia and BCG lymphadenitis present at the start of thalidomide therapy

A patient with intractable CGD colitis was treated with 1.5 mg/kg of thalidomide, while also taking 0.2 mg/kg oral corticosteroid and 1.5 mg/kg azathioprine. His bowel inflammatory lesions were located in colon and the clinical symptoms of colitis were evaluated using Pediatric Ulcerative Colitis Activity Index (PUCAI) scoring, a validated measurement of ulcerative colitis disease activity in children and adolescents [18]. Since thalidomide therapy was initiated, an improvement was seen in the symptoms of body weight loss and anemia and the disease activity by PUCAI (Figs. 5a and b). In line with his clinical improvements, his serum levels of TNF-α, IL-6, and IL-8 decreased at 6 to 8 weeks of thalidomide therapy (Fig. 5c), while serum IL-1β was undetectable during thalidomide therapy (data not shown). Regarding immune function, the number of $CD3^+$ T cells, $CD19^+$ B cells, and $CD4^+$ $CD45RA^+$ $CD31^+$ T cells that are thought to represent thymopoiesis increased after thalidomide therapy (Fig. 5d). The level of phytohemagglutinin-induced blastoid transformation was 33,300 cpm at 8 weeks of thalidomide treatment, which was within the normal range.

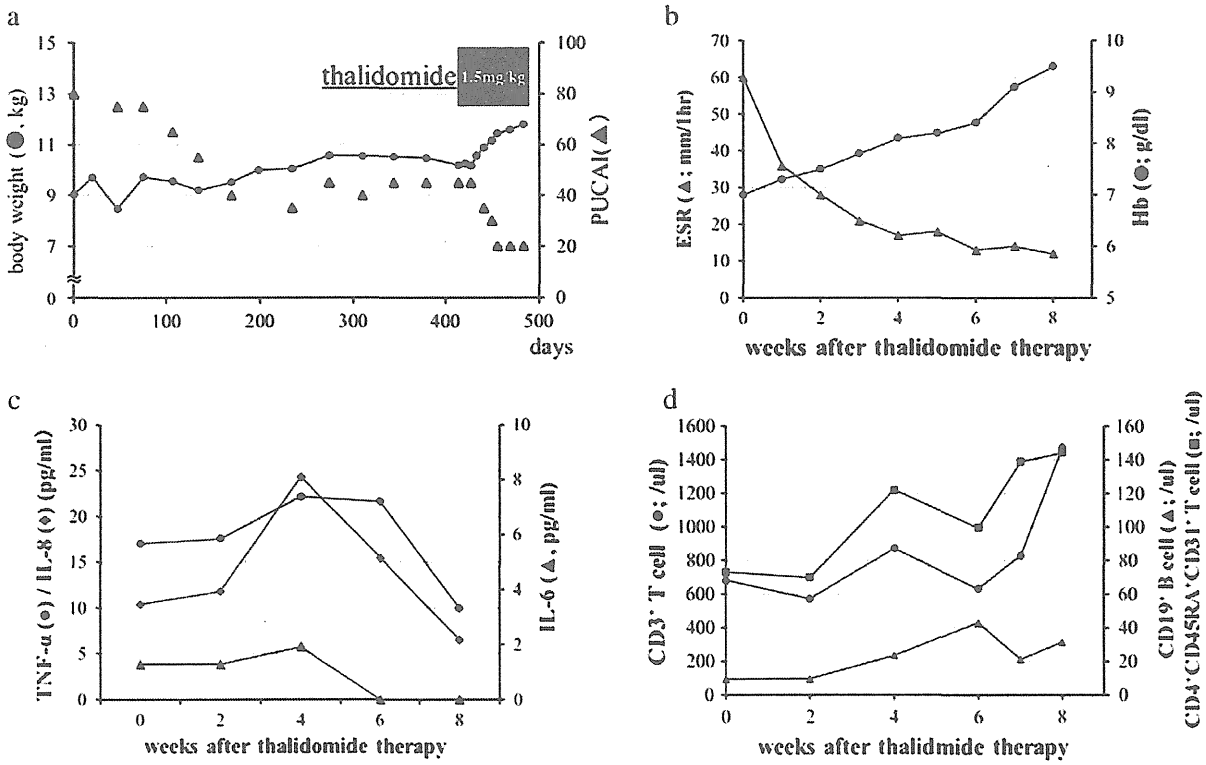

Figure 5 Thalidomide therapy improves symptoms of CGD colitis without immune suppression in a patient with CGD. A patient with CGD colitis received thalidomide therapy for 8 weeks. (a) After initiation of thalidomide therapy at day 421 of corticosteroid therapy, the patient gained 2 kg, and the pediatric ulcerative colitis activity index (PUCAI) improved from 45 to 20. (b) The erythrocyte sedimentation rate (triangles) decreased to 12 mm/h from 60 mm/h, and serum hemoglobin (circles) increased to 9.5 g/dl from 7 g/dl after 8 weeks of thalidomide therapy. (c) Serum levels of TNF-α (circles), IL-6 (triangles), and IL-8 (diamonds) decreased after 4 weeks of thalidomide therapy. (d) The number of $CD3^+$ T cells (circles), $CD4^+$ $CD45RA^+$ $CD31^+$ naïve T cells (squares), and $CD19^+$ B cells (triangles) in peripheral blood was analyzed by flow cytometry following thalidomide therapy.

The patient's pulmonary aspergillosis and *BCG*-related lymphadenitis that developed prior to thalidomide therapy were not aggravated and no other infections were identified during thalidomide therapy. Thalidomide treatment ceased at 8 weeks, and the conditioning for bone marrow transplantation was initiated next. The relapse of CGD colitis was completely eliminated by myeloablative conditioning and bone marrow transplantation after thalidomide therapy.

4. Discussion

The paradoxical clinical manifestations of CGD, susceptibility to infection and excessive inflammation, make it difficult to choose an appropriate course of therapy for patients with CGD colitis that develops through dysregulated inflammatory cytokine production [19–21]. The reason for this may be attributed to our insufficient understanding of a role for ROS on inflammasome activation. CGD patient monocytes were predisposed to secrete IL-1β in response to LPS, while CGD patients inherently lack NADPH oxidase activity in phagocytes. Furthermore, CGD monocytes stimulated with LPS activated caspase-1 comparable to those of healthy controls. These results suggest that ROS generated by NADPH oxidase were dispensable for NLRP3 inflammasome activation, or it seems to be more proper to say that ROS inhibit prolonged hyper-inflammation [22,23]. This hypothesis was also supported by results recently published [12]. They demonstrated that monocytes with p47phox deficiency activated caspase-1 and secreted IL-1β in response to LPS. Moreover, IL-1β secretion by CGD monocytes stimulated by uric acid crystals was 4-fold higher compared with that of healthy controls. Importantly, they showed that the small molecule diphenylene iodonium (DPI), an inhibitor of ROS, inhibited the production of TNF-α as well as IL-1β, and determined that DPI exerted the effects independently of the inflammasome. In the present study, we used the small molecule CCCP as an inhibitor of ROS generated by mitochondria and obtained similar results showing that CCCP inhibited production of inflammatory cytokines such as IL-1β, IL-6, IL-8, and TNF-α despite of no inhibition of caspase-1 activation. Together with the results of DPI, IL-1β production seems to be regulated by some mechanism other than the NLRP3 inflammasome. These underlying mechanisms that result in hyper-inflammation may explain why CGD patients frequently suffer from exaggerated bowel inflammation.

Unexpectedly, thalidomide did not show any inhibitory effects on the production of inflammatory cytokines in monocytes stimulated with LPS, but did inhibit the NF-κB activation when monocytes from CGD patients or healthy controls were stimulated with TNF-α. This curious difference has already been reported previously [15]. Although the mechanism remains unclear, thalidomide is considered to have partly negative effects on NF-κB signaling, showing anti-inflammatory activities [15]. Interestingly, while thalidomide has negative effects on NF-κB activation induced by TNF-α in a dose-dependent manner in hematopoietic and epithelial cells, the inhibitory effects were not observed in cells stimulated with LPS. The selective suppression of NF-κB by thalidomide is considered to be partly due to inhibition of an inhibitory subunit of NF-κB (IkBa), abrogation of IkBa activation, and inhibition of NF-κB-dependent reporter gene expression [15,24]. Furthermore, thalidomide inhibited IL-1β secretion in CGD monocytes that was augmented by addition of ATP in a dose-dependent manner, which was not observed in healthy controls. It is likely that thalidomide has some other pharmacological effects that diminish the exaggerated inflammatory environment that already existed in CGD monocytes [8]. Indeed, diminished inflammation due to thalidomide therapy was observed clinically in our patient with CGC colitis, who recovered following thalidomide therapy concomitant with decreases in serum inflammatory cytokines. Of importance was that the patient experienced no episodes of serious infection during short-term thalidomide therapy. Since granuloma formation is associated with dysregulated TNF-α production in inflammatory lesions [5], thalidomide, which selectively inhibits NF-κB activation induced by TNF-α, seems to be considered as a therapeutic option for patients with CGD colitis who are experiencing serious pathogenic infection.

Conflict of interest

The authors declare that they have no conflicts of interest.

Acknowledgments

We are grateful to the CGD patients and blood donors for their participation in this study. This work was supported by a Grant-in-Aid for Young Scientists (B) and a Grant from the National Center for Child Health and Development.

References

[1] F. Meissner, R.A. Seger, D. Moshous, A. Fischer, J. Reichenbach, A. Zychlinsky, Inflammasome activation in NADPH oxidase defective mononuclear phagocytes from patients with chronic granulomatous disease, Blood 116 (2010) 1570–1573.
[2] C. Dostert, V. Petrilli, R. Van Bruggen, C. Steele, B.T. Mossman, J. Tschopp, Innate immune activation through Nalp3 inflammasome sensing of asbestos and silica, Science 320 (2008) 674–677.
[3] T. Kawai, H. Kusakabe, A. Seki, S. Kobayashi, M. Onodera, Osteomyelitis due to trimethoprim/sulfamethoxazole-resistant *Edwardsiella tarda* infection in a patient with X-linked chronic granulomatous disease, Infection 39 (2011) 171–173.
[4] D.J. Marks, K. Miyagi, F.Z. Rahman, M. Novelli, S.L. Bloom, A.W. Segal, Inflammatory bowel disease in CGD reproduces the clinicopathological features of Crohn's disease, Am. J. Gastroenterol. 104 (2009) 117–124.
[5] G. Uzel, J.S. Orange, N. Poliak, B.E. Marciano, T. Heller, S.M. Holland, Complications of tumor necrosis factor-alpha blockade in chronic granulomatous disease-related colitis, Clin. Infect. Dis. 51 (2010) 1429–1434.
[6] C. Meierhofer, C.J. Wiedermann, New insights into the pharmacological and toxicological effects of thalidomide, Curr. Opin. Drug Discovery Devel. 6 (2003) 92–99.
[7] M. Keller, G. Sollberger, H.D. Beer, Thalidomide inhibits activation of caspase-1, J. Immunol. 183 (2009) 5593–5599.
[8] M. Eski, I. Sahin, M. Sengezer, M. Serdar, A. Ifran, Thalidomide decreases the plasma levels of IL-1 and TNF following burn injury: is it a new drug for modulation of systemic inflammatory response, Burns 34 (2008) 104–108.

[9] H. Sokol, F. Suarez, T. Meatchi, G. Malamut, M.A. Pocidalo, S. Blanche, C. Cellier, O. Hermine, Thalidomide as a treatment for refractory CGD colitis, Am. J. Gastroenterol. 104 (2009) 1069.
[10] M.A. Wallet, S.M. Wallet, G. Guiulfo, J.W. Sleasman, M.M. Goodenow, IFNgamma primes macrophages for inflammatory activation by high molecular weight hyaluronan, Cell. Immunol. 262 (2010) 84–88.
[11] M.G. Netea, C.A. Nold-Petry, M.F. Nold, L.A. Joosten, B. Opitz, J.H. van der Meer, F.L. van de Veerdonk, G. Ferwerda, B. Heinhuis, I. Devesa, C.J. Funk, R.J. Mason, B.J. Kullberg, A. Rubartelli, J.W. van der Meer, C.A. Dinarello, Differential requirement for the activation of the inflammasome for processing and release of IL-1beta in monocytes and macrophages, Blood 113 (2009) 2324–2335.
[12] F.L. van de Veerdonk, S.P. Smeekens, L.A. Joosten, B.J. Kullberg, C.A. Dinarello, J.W. van der Meer, M.G. Netea, Reactive oxygen species-independent activation of the IL-1beta inflammasome in cells from patients with chronic granulomatous disease, Proc. Natl. Acad. Sci. U. S. A. 107 (2010) 3030–3033.
[13] R. Zhou, A.S. Yazdi, P. Menu, J. Tschopp, A role for mitochondria in NLRP3 inflammasome activation, Nature 469 (2011) 221–225.
[14] J. Liobikas, D. Majiene, S. Trumbeckaite, L. Kursvietiene, R. Masteikova, D.M. Kopustinskiene, A. Savickas, J. Bernatoniene, Uncoupling and antioxidant effects of ursolic acid in isolated rat heart mitochondria, J. Nat. Prod. 74 (2011) 1640–1644.
[15] S. Majumdar, B. Lamothe, B.B. Aggarwal, Thalidomide suppresses NF-kappa B activation induced by TNF and H2O2, but not that activated by ceramide, lipopolysaccharides, or phorbol ester, J. Immunol. 168 (2002) 2644–2651.
[16] L. Franchi, R. Munoz-Planillo, G. Nunez, Sensing and reacting to microbes through the inflammasomes, Nat. Immunol. 13 (2012) 325–332.
[17] P. Pelegrin, A. Surprenant, Pannexin-1 mediates large pore formation and interleukin-1beta release by the ATP-gated P2X7 receptor, EMBO J. 25 (2006) 5071–5082.
[18] D. Turner, A.R. Otley, D. Mack, J. Hyams, J. de Bruijne, K. Uusoue, T.D. Walters, M. Zachos, P. Mamula, D.E. Beaton, A.H. Steinhart, A.M. Griffiths, Development, validation, and evaluation of a pediatric ulcerative colitis activity index: a prospective multicenter study, Gastroenterology 133 (2007) 423–432.
[19] K. Yasui, N. Uchida, Y. Akazawa, S. Nakamura, I. Minami, Y. Amano, T. Yamazaki, Thalidomide for treatment of intestinal involvement of juvenile-onset Behcet disease, Inflamm. Bowel. Dis. 14 (2008) 396–400.
[20] S. Malik, S.C. Wong, J. Bishop, K. Hassan, P. McGrogan, S.F. Ahmed, R.K. Russell, Improvement in growth of children with Crohn disease following anti-TNF-alpha therapy can be independent of pubertal progress and glucocorticoid reduction, J. Pediatr. Gastroenterol. Nutr. 52 (2011) 31–37.
[21] T. Olsen, R. Goll, G. Cui, I. Christiansen, J. Florholmen, TNF-alpha gene expression in colorectal mucosa as a predictor of remission after induction therapy with infliximab in ulcerative colitis, Cytokine 46 (2009) 222–227.
[22] E. Hatanaka, B.T. Carvalho, A. Condino-Neto, A. Campa, Hyperresponsiveness of neutrophils from gp 91phox deficient patients to lipopolysaccharide and serum amyloid A, Immunol. Lett. 94 (2004) 43–46.
[23] B.H. Segal, W. Han, J.J. Bushey, M. Joo, Z. Bhatti, J. Feminella, C.G. Dennis, R.R. Vethanayagam, F.E. Yull, M. Capitano, P.K. Wallace, H. Minderman, J.W. Christman, M.B. Sporn, J. Chan, D.C. Vinh, S.M. Holland, L.R. Romani, S.L. Gaffen, M.L. Freeman, T.S. Blackwell, NADPH oxidase limits innate immune responses in the lungs in mice, PLoS One 5 (2010) e9631.
[24] J.A. Keifer, D.C. Guttridge, B.P. Ashburner, A.S. Baldwin Jr., Inhibition of NF-kappa B activity by thalidomide through suppression of IkappaB kinase activity, J. Biol. Chem. 276 (2001) 22382–22387.

PLOS ONE

Gene Therapy Model of X-linked Severe Combined Immunodeficiency Using a Modified Foamy Virus Vector

Satoshi Horino[1,2], Toru Uchiyama[2], Takanori So[1], Hiroyuki Nagashima[1], Shu-lan Sun[1], Miki Sato[2], Atsuko Asao[1], Yoichi Haji[1], Yoji Sasahara[2], Fabio Candotti[3], Shigeru Tsuchiya[2], Shigeo Kure[2], Kazuo Sugamura[4], Naoto Ishii[1]*

1 Department of Microbiology and Immunology, Tohoku University Graduate School of Medicine, Sendai, Japan, 2 Department of Pediatrics, Tohoku University Graduate School of Medicine, Sendai, Japan, 3 Genetics and Molecular Biology Branch, National Human Genome Research Institute, National Institutes of Health, Bethesda, Maryland, United States of America, 4 Miyagi Cancer Center, Natori, Japan

Abstract

X-linked severe combined immunodeficiency (SCID-X1) is an inherited genetic immunodeficiency associated with mutations in the common cytokine receptor γ chain (γc) gene, and characterized by a complete defect of T and natural killer (NK) cells. Gene therapy for SCID-X1 using conventional retroviral (RV) vectors carrying the γc gene results in the successful reconstitution of T cell immunity. However, the high incidence of vector-mediated T cell leukemia, caused by vector insertion near or within cancer-related genes has been a serious problem. In this study, we established a gene therapy model of mouse SCID-X1 using a modified foamy virus (FV) vector expressing human γc. Analysis of vector integration in a human T cell line demonstrated that the FV vector integration sites were significantly less likely to be located within or near transcriptional start sites than RV vector integration sites. To evaluate the therapeutic efficacy, bone marrow cells from γc-knockout (γc-KO) mice were infected with the FV vector and transplanted into γc-KO mice. Transplantation of the FV-treated cells resulted in the successful reconstitution of functionally active T and B cells. These data suggest that FV vectors can be effective and may be safer than conventional RV vectors for gene therapy for SCID-X1.

Citation: Horino S, Uchiyama T, So T, Nagashima H, Sun S-l, et al. (2013) Gene Therapy Model of X-linked Severe Combined Immunodeficiency Using a Modified Foamy Virus Vector. PLoS ONE 8(8): e71594. doi:10.1371/journal.pone.0071594

Editor: Lishomwa C. Ndhlovu, University of Hawaii, United States of America

Received June 3, 2013; **Accepted** July 8, 2013; **Published** August 21, 2013

Funding: This study was supported in part by a grant-in-aid (#24659487 and #24390118) for scientific research on priority areas from the Ministry of Education, Science, Sports and Culture of Japan, a grant-in-aid for scientific research on priority areas from the Japan Society for the Promotion of Science, and grants (#111020001010004100) from the Japan Science and Technology Agency. The funders had no role in study design, data collection and analysis, decision to publish, or preparation of the manuscript. No additional external funding was received for this study.

Competing Interests: The authors have declared that no competing interests exist.

* E-mail: ishiin@med.tohoku.ac.jp

Introduction

X-linked severe combined immunodeficiency (SCID-X1) is a life-threatening immunodeficiency disorder, characterized by defective T and natural killer (NK) cell production and the development of functionally impaired B cells that lack the capacity to produce immunoglobulins. These defects result in a profound reduction in the development of both cellular and humoral immunity. SCID-X1 is caused by inactivating mutations in the gene encoding the cytokine receptor γ chain (γc), a common subunit of the receptors for interleukin (IL)-2, IL-4, IL-7, IL-9, IL-15, and IL-21 [1]. Bone marrow transplantation (BMT) from human leukocyte antigen (HLA)-identical siblings can cure the disease with a success rate of approximately 90%. However, BMT from non-HLA-identical donors results in lower survival rates due to a high risk for complications such as graft-versus-host disease, graft rejection, and incomplete T cell engraftment [2,3]. Consequently, gene therapy approaches have been developed as an alternative treatment option for those patients lacking appropriate donors.

The first gene therapy clinical trial for SCID-X1 was carried out by a French group in 1999 [4,5]. In that study, a conventional retroviral (RV) vector expressing γc was used, and resulted in the reconstitution of T and NK cell populations, and the recovery of humoral immunity. However, over time, acute T cell leukemia developed in 5 of the 20 patients receiving the therapy. The leukemia cells of these patients showed aberrant and high expressions of proto-oncogenes such as *LMO2*, which were caused by RV insertions within or near these loci [4,5]. To reduce the risk of vector-mediated insertional mutagenesis, various types of new vectors have since been developed [6,7].

Foamy virus (FV) is a non-pathogenic retrovirus belonging to the spumavirus genus and has unique biological characteristics, such as a wide host range (including humans), and wide tissue tropism [8,9]. Refined FV vectors that have large packaging capacities and are able to transduce murine and human hematopoietic stem cells (HSCs) have been reported [10–12]. In addition, FV vectors are reported to have a reduced tendency to integrate within or adjacent to the coding regions of genes compared to RV vectors. Due to these advantages, FV vectors have recently been used to correct genetic deficiencies in hematopoietic stem cells (HSCs) in several mouse models; these diseases include Wiskott–Aldrich syndrome (WAS) [13], leukocyte adhesion deficiency [14], Fanconi anemia [15], β-thalassemia [16], and X-linked chronic granulomatous disease [17].

In the present study, we evaluated the rate of insertional mutagenesis by a γc-FV vector compared to that of an RV vector in human T cells, and demonstrated the effectiveness of the γc-FV vector in a murine gene therapy model of SCID-X1.

Methods

All procedures were performed according to the protocols approved by the Institutional Committee for Use and Care of Laboratory Animals of Tohoku University, which was granted by Tohoku University Ethics Review Board (No. 2010MA165) and the Guide for Care and Use of Laboratory Animals published by the U.S. National Institutes of Health (NIH publication 85–23, revised 1996).

FV vector construction and production

FV vector plasmids were constructed as previously described [13,18,19]. In brief, a 631-bp *BspEI* and *Tth111I* restriction fragment from the ubiquitously acting chromatin-opening element promoter from the human HNRPA2B1-CBX3 locus (UCOE631) was isolated and inserted into the pΔΦ vector plasmid together with either the human γc (*IL2RG*) or enhanced green fluorescent protein (EGFP) complementary DNA (cDNA) to generate FV-IL2RG and FV-EGFP (Fig. 1A).

FV particles were produced by transfecting 293T cells with the resultant gene transfer vector plasmids and three helper plasmids (pCiGS, pCiPS, and pCiES) using FuGENE HD (Roche Applied Science), as previously described [13]. Culture supernatants were harvested after 48 hours and concentrated by ultracentrifugation.

A γc RV vector was constructed by inserting the human γc cDNA into the multi-cloning site of pMX-IRES-EGFP. Retroviral particles were produced by transfecting into amphotropic retrovirus packaging cells (PLAT-A cells) with pMx-IL2RG-IRES-EGFP using FuGENE HD. Culture supernatants containing the RV vector particles were harvested after 48 hours.

Cell lines

A human T cell line, ED40515(–) [20], which lacks γc expression, and an ED40515(–)-derived transfectant with a γc gene, EDγ, were described previously [21,22]. These cell lines were cultured in RPMI1640 medium supplemented with 10% FCS.

Mice

The γc-KO mice were previously reported [23]. γc-KO mice on a NOD/scid background [24] were obtained from the Central Institute for Experimental Animals (CIEA, Kawasaki, Japan). They were housed under specific pathogen-free conditions in individually ventilated cages and supplied with sterile food, water, and bedding. All procedures were performed according to protocols approved by the Institutional Committee for the Use and Care of Laboratory Animals of Tohoku University (2011MA139).

Vector transduction and BMT

Lineage marker depleted (Lin^-) cells were purified from the bone marrow cells of male γc-KO mice using magnetic cell sorting. The purified cells were exposed to FV vectors in StemSpan medium (StemCell Technologies Japan, Tokyo) supplemented with stem cell factor (50 ng/ml), IL-3 (5 ng/ml), Flt-3 ligand (5 ng/ml), and IL-6 (10 ng/ml) (all from Wako Pure Chemical Industries, Tokyo, Japan) on CH-296 (Retronectin; Takara Shuzo, Otsu, Japan)-coated plates for 16 hours. The transduced cells ($1–3\times10^6$) were then transplanted intravenously into 120 rad-irradiated female γc-KO mice on a NOD/scid background of 6–8 weeks of age. Eight to 12 weeks after BMT, and the peripheral blood cells and splenocytes were analyzed.

The ED40515 cell lines were similarly transduced with FV or RV vectors, except that cytokines were not added.

Immunofluorescence staining

For fluorescence-activated cell sorting (FACS) analysis, peripheral blood cells and splenocytes were collected from the mice. After removing erythrocytes with a lysing buffer, the cells were stained with anti-CD3-allophycocyanin (APC), anti-CD4-APC, anti-CD8-phycoerythrin (PE), anti-NK1.1-PE, anti-B220-APC, and/or anti-IgM-PE monoclonal antibodies (mAbs). Stained cells

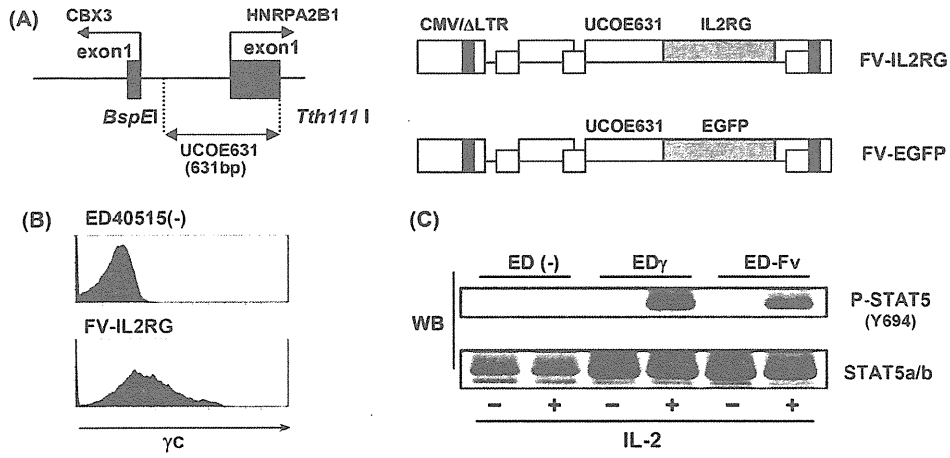

Figure 1. Structure and *in vitro* analysis of foamy virus vectors. (**A**) Structure of the foamy virus vectors. The UCOE631 promoter sequence from the human HNRPA2B1-CBX3 locus and transgenes were inserted into the FV vector. (**B**) Cell-surface expression of γc on ED40515(–) cells transduced with the FV-IL2RG vector. (**C**) STAT5 phosphorylation upon IL-2 stimulation. ED40515(–) cells, an ED40515(–)-derived transfectant with a γc gene, EDγ cells, and ED40515(–) cells transduced with the indicated vectors were stimulated with IL-2 for 30 min, and STAT5 phosphorylation in each cell line was detected by a STAT5 phosphospecific mAb.
doi:10.1371/journal.pone.0071594.g001

were analyzed with a FACS CantoII analyzer using the FACS Diva software (BD Biosciences, San Jose, CA).

Phosphorylated STAT5 detection

The IL-2-induced phosphorylation of STAT5 was detected by Western blotting as previously described [22]. In brief, cells were stimulated with 100 ng/ml IL-2 for 30 min at 37°C, collected, and lysed with a lysis buffer (20 mM Tris-HCl (pH 7.4), 150 mM NaCl, 2 mM EDTA, 1% NP-40, 50 mM NaF, 1 mM Na_3VO_4, and Protease Inhibitor Cocktail (Sigma-Aldrich Japan, Tokyo)). The protein lysates were separated by electrophoresis, transferred onto a polyvinylidene fluoride membrane, and blotted with STAT5 phosphospecific (pY694) antibodies (Cell Signaling Technology, Japan). Bound primary Abs were detected by a horseradish peroxidase-conjugated anti-rabbit IgG Ab followed by an enhanced chemiluminescence (ECL) detection reagent.

T cell proliferation and cytokine production

Spleen cells (1×10^5 cells/well) were stimulated with plate-coated anti-CD3 mAb (clone 2C11; 0.5 or 10 μg/ml) and/or 100 ng/ml recombinant human IL-2. T cell proliferation was measured after 48 hours by [^{3}H] thymidine incorporation and scintillation counting in triplicate. The stimulation index was calculated as the ratio of the incorporated radioactivity (cpm) of splenocytes from mice treated with FV-IL2RG-treated HSCs to that of splenocytes from mice treated with FV-EGFP-treated HSCs. IL-2 and IFN-γ production was assessed with an OptiEIA ELISA kit (BD Biosciences) after 24 hours and 72 hours, respectively, of stimulation, following the manufacturer's specifications.

Analysis of vector-insertion sites by ligation-mediated PCR

To determine the vector-integration sites, linker-mediated PCR was performed on genomic DNA isolated from γc-transduced ED40515(−) cells as previously described [13,25]. Briefly, the genomic DNA was digested with *Mse*I and *Pst*I, and the fragments were ligated to an MseI linker (5′-GTAATACGACTCACTA-TAGGGCTCCGCTTAAGGGACGAGGCGAATTCCCT-GAT-3′, 5′-PO4-TAGTCCCTTAAGCGGAG-NH2-3′). PCR was then performed with a linker-specific primer 5′-GTAATAC-GACTCACTATAGGGC-3′, and an FV long-terminal repeat-specific primer 5′-GTCTATGAGGAGCAGG AGTA-3′ or an RV long-terminal repeat-specific primer 5′-TAACCAAT-CAGTTCGCTTCTCGCTT-3′. A nested PCR was then performed using a linker-specific primer 5′-AGGGCTCCGCT-TAAGGGAC-3′, and an FV long-terminal repeat-specific primer 5′-CCTCCTTCCCTGTAATAGTC-3′ or an RV long-terminal repeat-specific primer 5′-CTCAATAAAAGAGCCCA-CAACCCC-3′. The PCR products were subcloned into pCR2.1 using the TOPO cloning kit (Life Technologies Japan, Tokyo), and the vector/DNA junction sites were sequenced with an ABI 3100 Genetic Analyzer (Applied Biosystems). The recovered vector/DNA junctions were matched to the human genome using the BLAT software program and each insertion locus was identified. Since integration sites of conventional RV vectors are preferentially found within 15 kb of transcriptional start sites (TSS) [26,27], we calculated the percentages of all integration sites within 15 kb of TSS. The integration frequency was calculated as previously described [28]. In brief, FV vector integration sites were mapped relative to RefSeq gene transcription start sites, binned into different size sequence windows, and plotted as the percent of all integrations per kb. Genes within 30 kb of the integration sites were also compared to the list of annotated cancer genes in the Atlas of Genetics and Cytogenetics in the Oncology and Hematology database (http://atlasgeneticsoncology.org/).

Statistical analysis

Statistical analysis was performed using χ^2-test or Student's t-test. P-values <0.05 were considered significant.

Results

FV vector performance in human T cells

We constructed two FV vectors, FV-IL2RG and FV-EGFP, to express human γc and EGFP, respectively, both of which were driven by the ubiquitously acting chromatin-opening element promoter (Fig. 1A, and see Materials and Methods). This promoter consists of a methylation-free CpG island without classic enhancer activity. To evaluate the function of the FV-IL2RG vector-expressed γc chain, we infected ED40515(−), a human T cell line lacking γc [21,22], with the FV vectors. A flow cytometric analysis detected clear γc expression on the surface of the FV-IL2RG-treated cells (Fig. 1B). Western blot analysis showed the phosphorylation of Stat5 upon IL-2 stimulation, reflecting the activation of intracellular signaling through the vector-mediated γc (Fig. 1C), and indicating the expression of functional γc. These results indicated that FV vectors can effectively transfer and express the γc gene in human T cells.

Profile of provirus integration sites in human T cells

We identified 100 independent integration sites of the FV or RV provirus in ED40515(−) cells infected with each vector, using a standard linker-mediated PCR analysis. Fig. 2A shows that the frequency of integration sites located within gene transcriptional units was comparable between the FV (36%) and RV (42%) vectors. However, the FV integration sites showed a significantly lower likelihood (13%) of being located immediately up or downstream of transcriptional start sites than the RV integration sites (25%) (Fig. 2A). Furthermore, the FV integration sites in the human T cells showed only a modest preference for regions near transcriptional start sites compared to RV integration sites (Fig. 2B), consistent with the results of previous studies [13,25,29].

In addition, we examined the cancer-related genes located within 30 kb of the FV and RV integration sites because all the RV insertion sites in gene therapy-related leukemia were shown within gene or within 30 kb of TSS of LMO-2 or BMI1 [30]. One of the 100 FV integration sites was detected inside the cancer-related gene, TCF12, which is known as a negative regulator of cell proliferation, whereas three of the RV integration sites were detected within cancer-related genes, (Klf5, NUMB, and FHIT) all of which are known leukemia-related genes.

Collectively, these results suggest that FV vectors might have a lower risk of vector-mediated genotoxicity than conventional RV vectors.

In vivo assessment of T cell restoration after FV-mediated gene therapy

To evaluate the efficacy of FV vector-mediated γc expression *in vivo*, we performed BMT experiments. Bone marrow Lin$^-$ cells from γc-KO mice were transduced with FV-IL2RG or FV-EGFP vectors. The cellular transduction efficiency of both vectors was between 33 and 40%. The FV vector-infected cells were intravenously transplanted into γc-KO mice on a NOD/scid background. Since older γc-KO mice on a C57BL/6 background were found to contain CD3$^+$CD4$^+$ cells (data not shown), γc-KO

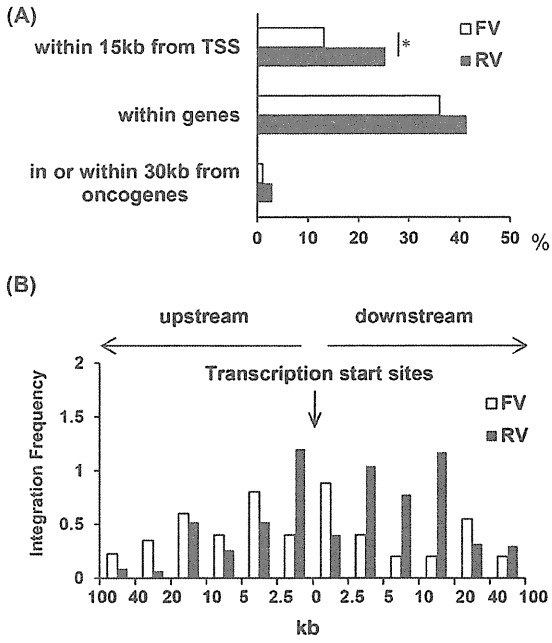

Figure 2. Profile of provirus integration in transduced cells. (A) Position of FV and RV integration sites. The percentage of all integration sites within 15 kb of transcriptional start sites, within genes that contain putative microRNA genes, and within 30 kb of oncogenes is shown for FV vector- or RV vector-treated cells. *$p<0.05$, χ^2-test. (B) A 100-kb window centered on TSS in the RefSeq database is shown. Relative frequencies of FV and RV vector integrations in each interval were calculated by dividing the percentage of integration b the indicated interval length.
doi:10.1371/journal.pone.0071594.g002

mice on a NOD/scid background were deemed a more suitable recipient for evaluating T cell reconstitution.

Eight weeks after transplantation, T cells emerged in the peripheral blood of the FV-IL2RG-treated group, and the clear expression of γc was confirmed on $CD8^+$ T cells (Fig. 3A). Gene therapy mice showed the recovery of CD4 and CD8 T cells as well as $B220^+$ IgM^+ B cells in spleen (in Figure 3B) although we could not detect NK cells. In addition, serum levels of IgM, IgG, and IgA were significantly elevated in FV-IL2RG-treated mice (Fig. 3C). These results indicate that HSCs transduced with FV-IL2RG have the potential for normal B and T cell differentiation.

We next investigated the functional capacity of the reconstituted T cells. Splenocytes from FV-IL2RG-treated mice showed proliferative responses following treatment with an anti-CD3 mAb, while those from the FV-EGFP-treated group did not (Fig. 4A). IL-2 stimulation induced proliferation through γc-transduced signals in T cells from FV-IL2RG-treated mice although stimulation with anti-CD3 mAb plus IL-2 did not enhance T cell proliferation compared to anti-CD3 mAb alone (Fig. 4A). The reconstituted T cells also produced IL-2 and IFN-γ upon stimulation with anti-CD3 mAb (Fig. 4B), indicating the functional restoration of T cells. Collectively, FV vector-mediated γc gene transfer was demonstrated to restore T and B cell differentiation and function *in vivo*.

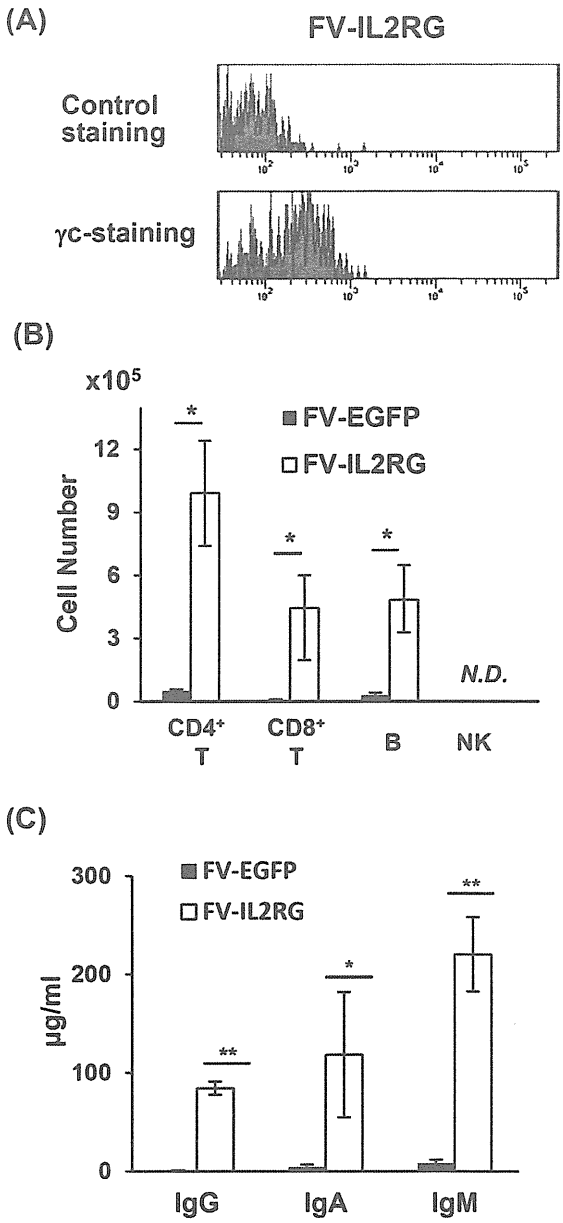

Figure 3. Reconstitution of T and B cells. (A) Cell-surface expression of γc on peripheral $CD8^+$ T cells in γc-KO mice treated with FV-IL2RG-treated HSCs. The upper and lower panels show isotype-control and γc-specific stainings, respectively. (B) The absolute numbers of $CD4^+$ T, $CD8^+$ T, $sIgM^+$ B, and NK cells in the spleen of γc-KO mice treated with FV-EGFP and FV-IL2RG ($n=4$ in each group). *N.D.*, not detectable. (C) Serum IgM, IgG, and IgA in FV-IL2RG-treated mice. Serum levels of IgM, IgG, and IgA were measured by ELISA. Results shown are the mean ± SD of the stimulation index from 4 mice in each group. *$p<0.05$ and **$p<0.01$, Student t-test.
doi:10.1371/journal.pone.0071594.g003

Discussion

Vector-mediated insertional mutagenesis is a critical problem associated with conventional RV-mediated gene therapy treatments for SCID-X1. To address this issue, we developed a

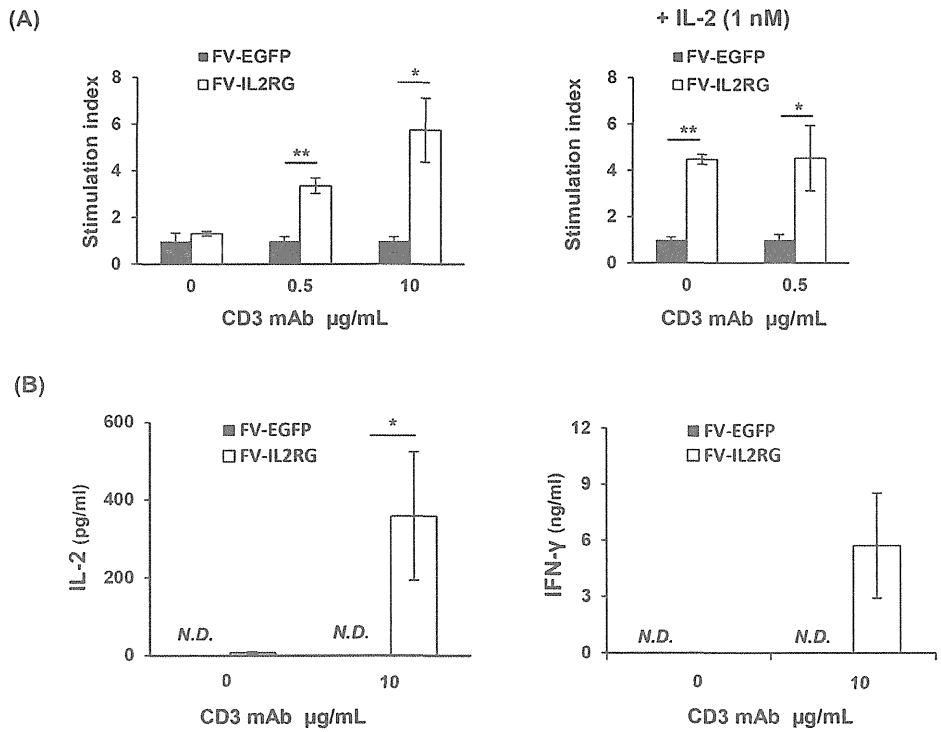

Figure 4. In vitro function of reconstituted T cells. (A) Splenocytes from recipient mice were stimulated with an anti-CD3 mAb at the indicated dose in the presence (right) or absence (left) of IL-2. Results shown are the mean ± SD of the stimulation index from 4 or 5 mice in each group. *p<0.05 and **p<0.01, Student t-test. (B) IL-2 and IFN-γ production by reconstituted T cells. Splenocytes from recipient mice were stimulated with an anti-CD3 mAb at the indicated dose. Culture supernatants were collected 24 and 72 hours after stimulation. Concentration of each cytokine in the supernatant was measured by ELISA. Results shown are the mean ± SD from 4 mice in each group. *p<0.05, Student t-test. *N.D.*, not detectable.
doi:10.1371/journal.pone.0071594.g004

modified FV vector carrying the human γc gene, and evaluated the vector-mediated insertional mutagenesis as well as the *in vivo* T, B, and NK cell reconstitution. Our findings demonstrated that the integration sites of the FV vector were significantly less likely to be located within or near transcriptional start sites compared to those of a conventional RV vector, suggesting that the FV vector had a lower risk for insertion-mediated genotoxicity. We also showed the successful reconstitution of functionally active T and B cells after the transplantation of HSCs containing a γc-FV vector into γc-KO recipient mice. This is the first reported use of an FV vector in a gene therapy mouse model of SCID-X1.

Previous studies showed that the use of classical RV vector for SCID-X1 gene therapy resulted in the development of leukemia in a number of patients [4,5]. The leukemogenesis associated with these vectors is likely to be due to inappropriate vector insertion in or near proto-oncogenes. Consistent with previous reports that FV vectors have a more random genomic integration pattern than RV vectors [28], our data indicated that the FV vector integration sites were less likely to be near transcription start sites than those of RV vectors (Fig. 2A, 2B). In addition, three integration sites of the RV vector were found within cancer-related genes (Klf5, NUMB, and FHIT), all of which are associated with leukemogenesis or leukemia progression [31–33]. Although one FV vector integration site was found within a cancer-related gene, TCF12, no evidence showing a relationship between TCF12 and leukemogenesis has been reported. These results are consistent with the accepted theory that FV is non-pathogenic for humans [8,9], and support the notion that FV vectors may be safer than conventional RV vectors.

The main objective of SCID-X1 gene therapy is the robust reconstitution of T, B, and NK cells. However, in the present study, use of the FV-IL2RG vector failed to reconstitute the NK cell population when monitored up to 4 months after gene therapy. One possible explanation for this deficiency may be that the human γc gene is not entirely compatible with the mouse system. Consistent with our findings, impaired NK cell reconstitution in mouse SCID-X1 gene therapy using the human γc gene was previously reported [34]; however, gene therapies in mouse models with RV vectors carrying the mouse γc gene were shown to reconstitute NK cells within two months [35–37]. NK cell development requires IL-15, while the differentiation and survival of T and B cells require IL-7. Receptors for both cytokines contain the shared γc subunit [1]. Therefore, the human γc might function less effectively as a mouse IL-15 receptor subunit than as a mouse IL-7 receptor subunit. In addition, T cell responses to IL-2 might also be insufficient as additional stimulation of IL-2 did not increase the T cell response with anti-CD3 mAb alone. Namely, the chimeric IL-2 and IL-15 receptors consisting of mouse α and β chains in combination with human γc might not fully function as a physiological mouse IL-2 and IL-15 receptors, respectively. In any case, the use of human γc, rather than the FV vector, is the probable cause of the impaired NK cell reconstitution and possible insufficient T cell function in this study.

We recently reported the successful treatment of a WAS mouse model using gene therapy with an FV vector [13]. Similar to

SCID-X1, the gene therapy for WAS requires T cell proliferative and functional restoration. Our studies collectively support the potential for modified FV vector-mediated gene therapy for the successful treatment of T cell immunodeficiencies. Moreover, FV vectors have also been shown to be effective for the treatment of red blood cell and granulocyte disorders in mouse models [14–17]. Based on their broad host range and ability to efficiently transduce HSCs, FV vectors may be applicable in gene therapies for many different hematopoietic disorders.

Over the last decade, novel modifications of RV vectors have been developed to overcome the problems associated with SCID-X1 gene therapy. However, it is still controversial which vector is the most favorable for safety. FV vectors have the potential to increase the efficacy of HSC-based gene therapies and to reduce the risk of genotoxicity. Although further studies are necessary, our data support the potential clinical application of FV vectors in gene therapy for SCID-X1 in the future.

Acknowledgments

We sincerely thank Drs. David W. Russell (University of Washington) and Adrian J. Thrasher (University College of London) for sharing reagents. We also thank the Biomedical Research Core Animal Pathology Platform for the essential technical support of pathological analysis.

Author Contributions

Conceived and designed the experiments: NI TU. Performed the experiments: SH TS HN SLS MS AA YH. Analyzed the data: ST SK KS. Contributed reagents/materials/analysis tools: TU YS FC. Wrote the paper: NI SH TU.

References

1. Sugamura K, Asao H, Kondo M, Tanaka N, Ishii N, et al. (1996) The interleukin-2 receptor gamma chain: its role in the multiple cytokine receptor complexes and T cell development in XSCID. Annu Rev Immunol 14: 179–205.
2. Buckley RH, Schiff SE, Schiff RI, Markert L, Williams LW, et al. (1999) Hematopoietic stem-cell transplantation for the treatment of severe combined immunodeficiency. N Engl J Med 340: 508–516.
3. Haddad E, Landais P, Friedrich W, Gerritsen B, Cavazzana-Calvo M, et al. (1998) Long-term immune reconstitution and outcome after HLA-nonidentical T-cell-depleted bone marrow transplantation for severe combined immunodeficiency: a European retrospective study of 116 patients. Blood 91: 3646–3653.
4. Fischer A, Hacein-Bey-Abina S, Cavazzana-Calvo M (2010) 20 years of gene therapy for SCID. Nat Immunol 11: 457–460.
5. Cavazzana-Calvo M, Fischer A (2007) Gene therapy for severe combined immunodeficiency: are we there yet? J Clin Invest 117: 1456–1465.
6. Montini E, Cesana D, Schmidt M, Sanvito F, Bartholomae CC, et al. (2009) The genotoxic potential of retroviral vectors is strongly modulated by vector design and integration site selection in a mouse model of HSC gene therapy. J Clin Invest 119: 964–975.
7. Modlich U, Navarro S, Zychlinski D, Maetzig T, Knoess S, et al. (2009) Insertional transformation of hematopoietic cells by self-inactivating lentiviral and gammaretroviral vectors. Mol Ther 17: 1919–1928.
8. Russell DW, Miller AD (1996) Foamy virus vectors. J Virol 70: 217–222.
9. Stirnnagel K, Luftenegger D, Stange A, Swiersy A, Mullers E, et al. (2010) Analysis of prototype foamy virus particle-host cell interaction with autofluorescent retroviral particles. Retrovirology 7: 45.
10. Vassilopoulos G, Trobridge G, Josephson NC, Russell DW (2001) Gene transfer into murine hematopoietic stem cells with helper-free foamy virus vectors. Blood 98: 604–609.
11. Josephson NC, Trobridge G, Russell DW (2004) Transduction of long-term and mobilized peripheral blood-derived NOD/SCID repopulating cells by foamy virus vectors. Hum Gene Ther 15: 87–92.
12. Leurs C, Jansen M, Pollok KE, Heinkelein M, Schmidt M, et al. (2003) Comparison of three retroviral vector systems for transduction of nonobese diabetic/severe combined immunodeficiency mice repopulating human CD34+ cord blood cells. Hum Gene Ther 14: 509–519.
13. Uchiyama T, Adriani M, Jagadeesh GJ, Paine A, Candotti F (2012) Foamy virus vector-mediated gene correction of a mouse model of Wiskott-Aldrich syndrome. Mol Ther 20: 1270–1279.
14. Bauer TR Jr, Allen JM, Hai M, Tuschong LM, Khan IF, et al. (2008) Successful treatment of canine leukocyte adhesion deficiency by foamy virus vectors. Nat Med 14: 93–97.
15. Si Y, Pulliam AC, Linka Y, Ciccone S, Leurs C, et al. (2008) Overnight transduction with foamyviral vectors restores the long-term repopulating activity of Fancc−/− stem cells. Blood 112: 4458–4465.
16. Morianos I, Siapati EK, Pongas G, Vassilopoulos G (2012) Comparative analysis of FV vectors with human alpha- or beta-globin gene regulatory elements for the correction of beta-thalassemia. Gene Ther 19: 303–311.
17. Chatziandreou I, Siapati EK, Vassilopoulos G (2011) Genetic correction of X-linked chronic granulomatous disease with novel foamy virus vectors. Exp Hematol 39: 643–652.
18. Trobridge G, Josephson N, Vassilopoulos G, Mac J, Russell DW (2002) Improved foamy virus vectors with minimal viral sequences. Mol Ther 6: 321–328.
19. Zhang F, Thornhill SI, Howe SJ, Ulaganathan M, Schambach A, et al. (2007) Lentiviral vectors containing an enhancer-less ubiquitously acting chromatin opening element (UCOE) provide highly reproducible and stable transgene expression in hematopoietic cells. Blood 110: 1448–1457.
20. Arima N, Kamio M, Imada K, Hori T, Hattori T, et al. (1992) Pseudo-high affinity interleukin 2 (IL-2) receptor lacks the third component that is essential for functional IL-2 binding and signaling. J Exp Med 176: 1265–1272.
21. Ishii N, Asao H, Kimura Y, Takeshita T, Nakamura M, et al. (1994) Impairment of ligand binding and growth signaling of mutant IL-2 receptor gamma-chains in patients with X-linked severe combined immunodeficiency. J Immunol 153: 1310–1317.
22. Asao H, Okuyama C, Kumaki S, Ishii N, Tsuchiya S, et al. (2001) Cutting edge: the common gamma-chain is an indispensable subunit of the IL-21 receptor complex. J Immunol 167: 1–5.
23. Ohbo K, Suda T, Hashiyama M, Mantani A, Ikebe M, et al. (1996) Modulation of hematopoiesis in mice with a truncated mutant of the interleukin-2 receptor gamma chain. Blood 87: 956–967.
24. Ito M, Hiramatsu H, Kobayashi K, Suzue K, Kawahata M, et al. (2002) NOD/SCID/gamma(c)(null) mouse: an excellent recipient mouse model for engraftment of human cells. Blood 100: 3175–3182.
25. Wu X, Li Y, Crise B, Burgess SM (2003) Transcription start regions in the human genome are favored targets for MLV integration. Science 300: 1749–1751.
26. Laufs S, Nagy KZ, Giordano FA, Hotz-Wagenblatt A, Zeller WJ, et al. (2004) Insertion of retroviral vectors in NOD/SCID repopulating human peripheral blood progenitor cells occurs preferentially in the vicinity of transcription start regions and in introns. Mol Ther 10: 874–881.
27. Montini E, Cesana D, Schmidt M, Sanvito F, Ponzoni M, et al. (2006) Hematopoietic stem cell gene transfer in a tumor-prone mouse model uncovers low genotoxicity of lentiviral vector integration. Nat Biotechnol 24: 687–696.
28. Trobridge GD, Miller DG, Jacobs MA, Allen JM, Kiem HP, et al. (2006) Foamy virus vector integration sites in normal human cells. Proc Natl Acad Sci U S A 103: 1498–1503.
29. Beard BC, Keyser KA, Trobridge GD, Peterson LJ, Miller DG, et al. (2007) Unique integration profiles in a canine model of long-term repopulating cells transduced with gammaretrovirus, lentivirus, or foamy virus. Hum Gene Ther 18: 423–434.
30. Hacein-Bey-Abina S, Garrigue A, Wang GP, Soulier J, Lim A, et al. (2008) Insertional oncogenesis in 4 patients after retrovirus-mediated gene therapy of SCID-X1. J Clin Invest 118: 3132–3142.
31. Zhu N, Gu L, Findley HW, Chen C, Dong JT, et al. (2006) KLF5 Interacts with p53 in regulating survivin expression in acute lymphoblastic leukemia. J Biol Chem 281: 14711–14718.
32. Ito T, Kwon HY, Zimdahl B, Congdon KL, Blum J, et al. (2010) Regulation of myeloid leukaemia by the cell-fate determinant Musashi. Nature 466: 765–768.
33. Stam RW, den Boer ML, Passier MM, Janka-Schaub GE, Sallan SE, et al. (2006) Silencing of the tumor suppressor gene FHIT is highly characteristic for MLL gene rearranged infant acute lymphoblastic leukemia. Leukemia 20: 264–271.
34. Huston MW, van Til NP, Visser TP, Arshad S, Brugman MH, et al. (2011) Correction of murine SCID-X1 by lentiviral gene therapy using a codon-optimized IL2RG gene and minimal pretransplant conditioning. Mol Ther 19: 1867–1877.
35. Otsu M, Sugamura K, Candotti F (2000) In vivo competitive studies between normal and common gamma chain-defective bone marrow cells: implications for gene therapy. Hum Gene Ther 11: 2051–2056.
36. Otsu M, Sugamura K, Candotti F (2001) Lack of dominant-negative effects of a truncated gamma(c) on retroviral-mediated gene correction of immunodeficient mice. Blood 97: 1618–1624.
37. Kume A, Koremoto M, Mizukami H, Okada T, Hanazono Y, et al. (2002) Selective growth advantage of wild-type lymphocytes in X-linked SCID recipients. Bone Marrow Transplant 30: 113–118.

Molecular Genetics and Metabolism 111 (2014) 139–146

Contents lists available at ScienceDirect

Molecular Genetics and Metabolism

journal homepage: www.elsevier.com/locate/ymgme

Enzyme augmentation therapy enhances the therapeutic efficacy of bone marrow transplantation in mucopolysaccharidosis type II mice

Kazumasa Akiyama [a,b], Yohta Shimada [a], Takashi Higuchi [a], Makoto Ohtsu [c], Hiromitsu Nakauchi [c], Hiroshi Kobayashi [a,d], Takahiro Fukuda [e], Hiroyuki Ida [a,d], Yoshikatsu Eto [f], Brett E. Crawford [g], Jillian R. Brown [g], Toya Ohashi [a,d,*]

[a] Department of Gene Therapy, Institute of DNA Medicine, Research Center for Medical Sciences, The Jikei University School of Medicine, Tokyo, Japan
[b] Department of Pediatrics, Kitasato University Graduate School of Medicine, Kanagawa, Japan
[c] Division of Stem Cell Therapy, Center for Stem Cell and Regenerative Medicine, Institute of Medical Science, University of Tokyo, Tokyo, Japan
[d] Department of Pediatrics, The Jikei University School of Medicine, Tokyo, Japan
[e] Division of Neuropathology, Department of Pathology, The Jikei University School of Medicine, Tokyo, Japan
[f] Advanced Clinical Research Center, Institute of Neurological Disorders, Kanagawa, Japan
[g] BioMarin Pharmaceutical Inc., San Diego, CA, USA

ARTICLE INFO

Article history:
Received 5 August 2013
Received in revised form 17 September 2013
Accepted 17 September 2013
Available online 21 September 2013

Keywords:
Mucopolysaccharidosis
Bone marrow transplantation
Enzyme replacement therapy
Glycosaminoglycan
Pathologic glycosaminoglycan
Hunter syndrome

ABSTRACT

Before the availability of an enzyme replacement therapy (ERT) for mucopolysaccharidosis type II (MPS II), patients were treated by bone marrow transplantation (BMT). However, the effectiveness of BMT for MPS II was equivocal, particularly at addressing the CNS manifestations. To study this further, we subjected a murine model of MPS II to BMT and evaluated the effect at correcting the biochemical and pathological aberrations in the viscera and CNS. Our results indicated that BMT reduced the accumulation of glycosaminoglycans (GAGs) in a variety of visceral organs, but not in the CNS. With the availability of an approved ERT for MPS II, we investigated and compared the relative merits of the two strategies either as a mono or combination therapy. We showed that the combination of BMT and ERT was additive at reducing tissue levels of GAGs in the heart, kidney and lung. Moreover, ERT conferred greater efficacy if the immunological response against the infused recombinant enzyme was low. Finally, we showed that pathologic GAGs might potentially represent a sensitive biomarker to monitor the therapeutic efficacy of therapies for MPS II.

1. Introduction

Mucopolysaccharidosis type II (MPS II, Hunter syndrome) is an X-linked lysosomal storage disorder (LSD) caused by a deficiency in the activity of the lysosomal enzyme, iduronate-2-sulfate (IDS, EC 3.1.6.13), which degrades the glycosaminoglycans (GAGs), heparan sulfate and dermatan sulfate [1]. The widespread and progressive lysosomal accumulation of undegraded GAGs leads to a broad spectrum of clinical manifestations. These include skeletal deformities, cardiac valvular disease, cardiac hypertrophy, hepatosplenomegaly, coarse facial appearance, upper airway narrowing, hearing defect, enlarged tongue, retinopathy and CNS involvement [2]. These clinical symptoms significantly compromise the patients' quality of life.

Presently, two therapies are available to treat MPS II; one is enzyme replacement therapy (ERT) and the other is bone marrow transplantation (BMT). ERT has been shown to be effective at correcting aspects of the visceral disease [3–5] but not the CNS lesion as the enzyme dose not cross the blood–brain barrier [6,7]. ERT also has a limited impact on the bone and valvular lesions [8]. In addition, the need for repeated infusions of the enzyme is costly and confers a heavy burden on the MPS II patients [9].

BMT has been shown to be effective at treating several neuropathic LSDs such as MPS I, MPS VI, globoid-cell leukodystrophy, metachromatic leukodystrophy, Gaucher disease and others [10,11]. In contrast to ERT, BMT might address the CNS lesions associated with several LSDs by virtue of the migration of enzyme competent donor cells into the brain. Consequent secretion of the enzyme from these cells may allow for cross-correction of patients' enzyme deficient neuronal cells. Early studies suggested that BMT should not be indicated for MPS II patients due to disappointing outcomes, particularly the limited impact on CNS involvement [12–15]. However, recent report demonstrated the long-term efficacy of BMT in CNS involvement of an MPS II patient [16]. Thus, it is not evident if BMT should be indicated for MPS II. Moreover, there have been no animal studies showing the impact of BMT at reducing the level of GAGs in the brain.

Prior to the availability of ERT, some patients were treated by BMT with the hope of improving the visceral disease and CNS disease. Now

* Corresponding author at: 3-25-8 Nishishinbashi, Minato-ku, Tokyo 105-8461, Japan. Fax: +81 3 3433 1230.
E-mail address: tohashi@jikei.ac.jp (T. Ohashi).

1096-7192/$ – see front matter © 2013 Elsevier Inc. All rights reserved.
http://dx.doi.org/10.1016/j.ymgme.2013.09.013

that an approved enzyme is available for these patients, we asked if ERT could enhance the therapeutic effect of BMT. This has not been demonstrated for either human or murine MPS II. In this study, we examined the effectiveness of BMT at addressing CNS disease, as well as the relative merits of the combination of BMT and ERT in a mouse model of MPS II.

2. Methods

2.1. Animal husbandry

Female mice heterozygous for the X-linked allele ($IDS^{+/-}$) on a congenic C57BL/6 background were kindly provided from Joseph Muenzer (University of North Carolina, Chapel Hill) [17]. The carrier females were bred with male wild type (WT) mice of the same genetic background strain, producing hemizygous IDS knock-out males (MPS II mouse model, $IdS^{-/0}$). The genotypes of all offspring were determined by polymerase chain reaction analysis of DNA obtained from a tail snip. B6.SJL-ptprca mice congenic at the CD45 locus ($CD45.1^{+}CD45.2^{-}$) were purchased from Sankyo Labo Service (Tokyo, Japan), and bred with female C57BL/6 ($CD45.1^{-}CD45.2^{+}$) WT, producing C57BL/6 ($CD45.1^{+}CD45.2^{+}$) donor mice. These mice were used as donors. Animal husbandry and all procedures in the animal experiments were approved by The Animal Care Committee at The Jikei University School of Medicine.

2.2. BMT

BMT was performed as previously described with minor modification [18]. Bone marrow cells were harvested from femurs and tibias of male C57BL/6 ($CD45.1^{+}CD45.2^{+}$) mice (8–12 weeks of age). The bone marrow cells (2.0×10^{6}) were transplanted to lethally irradiated (9Gy) recipient MPS II mice intravenously. Irradiation was carried out using the Hitach-MBR1520R irradiator (Hitachi, Tokyo, Japan). To confirm engraftment, the peripheral blood was collected from treated mice (2 times: 12 weeks and 27 weeks after transplantation). Flow cytometric analysis was carried out using MACSQuant® Analyzer (Miltenyi Biotec, Bergisch Gladbach, Germany) and analyzed using MACSQuantify® Software (Miltenyi Biotec). Briefly, peripheral blood cells were stained with fluorescein isothiocyanate-conjugated anti-murine CD45.1 and allophycocyanin-conjugated anti-murine CD45.2 (eBioscience, San Diego, CA, USA). The each lineage was distinguished by using the corresponding phycoerythrin-conjugated antibody: (Bcell-CD45R, Tcell-CD3e, Granulocyte-Ly6G, Macrophage-CD11b, eBioscience). The donor-derived cell engraftment was determined as the percentage of $CD45.1^{+}CD45.2^{+}$ cells.

2.3. ERT

The MPS II mice were administered 0.5 mg/kg human IDS (Idursulfase, Shire HGT Pharmaceuticals, Cambridge, MA, USA, generously gifted from Genzyme Japan Co., Ltd. in Tokyo) via a tail vein once a week.

2.4. Therapeutic regimen

Therapeutic regimen was shown in Fig. 1. There are 3 treatment groups, BMT group, ERT group and BMT + ERT group. Control groups consisted with untreated MPS II mice and WT mice. In ERT group, ERT started at 9 weeks of age with total 27 times. In BMT group, BMT was carried out at 9 weeks of age. In BMT + ERT group, BMT was performed at 9 weeks of age and ERT was initiated at 12 weeks after BMT with total 15 times. All mice were measured the body weight and collected the blood and urine samples at various time points. In ERT and BMT + ERT groups, blood was harvested just prior to ERT every time. Y-maze test was carried out in all treatment groups at between 26 and 27 weeks after treatment, and sacrificed for tissue biochemical and pathological assays at 27 weeks after initiation of treatment. The mice in ERT and BMT + ERT groups sacrificed 1 week after last ERT.

2.5. Serum and tissue IDS activity

IDS activity was determined in serum and homogenized tissue, as previously described using the artificial substrate 4-methylumbelliferyl-alpha-iduronide-2-sulfate (MU-αIdu-2S) (Moscerdam Substrates, Oegstgeest, Netherlands) [19]. Protein concentrations were determined using the BCA protein assay kit (Thermo Fisher Scientific, IL, USA). The tissue IDS enzyme activity was expressed as nmol/4 h/mg protein. The serum IDS activity was expressed as % activity of WT mice.

2.6. Total GAGs assay

Total GAG (tGAG) concentration in urine and tissue extracts was quantified by the Wieslad® sGAG quantitative Alcian blue-binding assay kit (Euro-Diagnostica, Malmö, Sweden) as previously described [19]. The urine creatinine was assayed using a commercially available kit (Wako Pure Chemical Industries, Ltd., Osaka, Japan). The urinary and tissue GAG amount was expressed as μg GAG/mg creatinine and μg GAG/mg protein, respectively.

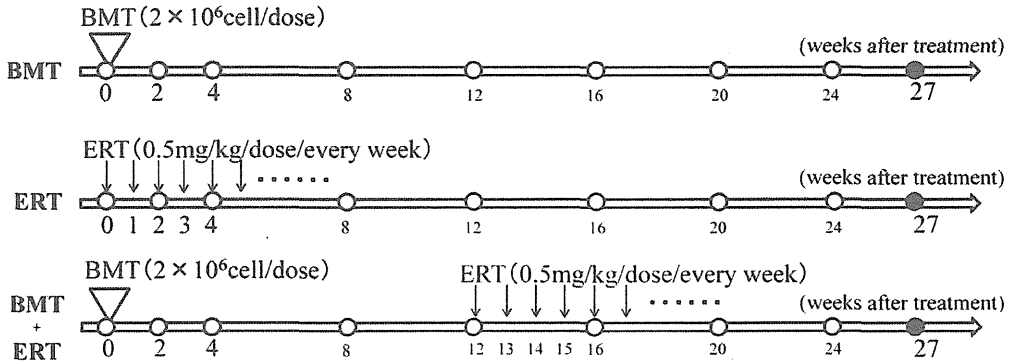

Fig. 1. Therapy experimental design. The picture shows diagram of therapeutic regimen. The therapeutic groups included BMT only, ERT only, and the combination of BMT and ERT in MPS II mice. Downward triangles mark the initiation of BMT. The solid arrows indicate IDS administration. Open circles mark time points of blood and urine collection for IDS activity, GAG detection, and anti-IDS antibody assays. The filled circles show the time point of sacrifice. In BMT groups, BMT was carried out at 9 weeks of age. In ERT group, ERT was initiated at 9 weeks of age followed by weekly infusion total 27 times. In ERT + BMT groups, BMT was carried out at 9 weeks of age and ERT was added 12 weeks after BMT. Thereafter, ERT was continued weekly for a total of 15 times. All mice were sacrificed 27 weeks after initiation of treatment.

2.7. Pathologic GAGs assay

The pathologic GAGs (pGAGs) assays were performed by using the Sensi-Pro Non-Reducing End (NRE) heparan sulfate assay as described [20]. The Sensi-Pro assay measures only lysosomal accumulated heparan sulfate caused by the deficient activity of IDS by specifically quantifying the 2-O sulfated non-reducing end derived after heparin lyase digestion. Briefly, tissue samples were homogenized and the GAGs were isolated by anion exchange chromatography and digested with heparin lyase (IBEX Technologies, Montreal, Canada). Enzymatically depolymerized MPS II specific NRE, 2-sulfoiduronic linked to N-sulfoglucosamine-6-sulfate (I2S6), tagged with [$^{12}C_6$] was measured according to standard curves of saturated heparan sulfate tagged with [$^{13}C_6$], derived commercially available standard unsaturated disaccharides. This measurement was performed by using Liquid Chromatography–Mass Spectrometry and the data were represented as average of triplicates.

2.8. Pathologically analysis

The mice were euthanized using pentobarbital and perfused with 4% paraformaldehyde and 2% glutaraldehyde (Wako Pure Chemical Industries, Ltd.) in 0.1 M PBS through the heart. The liver, heart, spleen and kidney were removed and immersed in the same fixative solution for a minimum of 2 h. Tissue samples were postfixed in 1% osmium tetroxide, and embedded in epoxy resin. The sections were cut at 1 μm thickness, stained with toluidine blue, and assessed to detect large distended lysosomes using light microscopy (BX50; Olympus Optical Co, Ltd., Tokyo, Japan).

2.9. Assay for rhIDS-specific IgG

IgG antibodies recognizing rhIDS were assayed using an enzyme-linked immunosorbent assay (ELISA). Briefly, 96-well plates Nunc-Immuno palate MaxiSorp® (Nunc, Roskilde, Denmark) were coated with 10 μg of rhIDS in PBS overnight at 4 °C. The plates were blocked by adding 100 μl PBS/1% bovine serum albumin and incubating for 5 h at room temperature. After this step, the wells were washed with PBS/0.05% Tween 20. The serum samples from mice were diluted 100-fold with PBS/1% bovine serum albumin, and 100 μl diluted serum was added to each well and incubated for 1 h at room temperature. The plate was then washed with the same buffer and reacted with 100 μl of 5000-fold diluted peroxidase-conjugated anti-mouse IgG Ab (Kirkegaard & Perry Labs, Gaithersburg, MA, USA). After incubation for 30 min at room temperature, the plates were washed again and color was generated by the addition of 3,3′,5′,5′-tetramethylbenzidine substrate reagent (Kirkegaard & Perry Labs) for 10 min at room temperature. The reaction was stopped by adding 100 μl of 0.6 N H_2SO_4, and the optical density was measured at 450 nm using an ARVOMX/Light plate reader (PerkinElmer, Waltham, MA, USA). The Ab titer was calculated using mouse anti-human IDS monoclonal antibody as a standard (generously gifted by JCR pharmaceutical Co., Ltd.).

2.10. Statistical analysis

Data were assessed using GraphPad Prism software (GraphPad software, Inc., La Jolla, CA, USA). T-test or one-way ANOVA with Tukey–Kramer's post test was used. Significance was considered to be $P < 0.05$.

3. Results

3.1. Engraftment of donor cells in mice treated with BMT and a combination of BMT and ERT

Donor cell engraftment in mice subjected to BMT and BMT + ERT was analyzed at 12 weeks and 27 weeks following BMT (Table 1).

Table 1
Donor-derived cell engraftment in each lineage in BMT and BMT + ERT groups.

	B cell (%)[a]	T cell (%)[a]	Granulocyte (%)[a]	Macrophage (%)[a]
12 weeks after BMT				
BMT	95.72 ± 4.51	78.99 ± 5.39	87.39 ± 4.64	89.6 ± 7.88
BMT + ERT	96.41 ± 1.64	79.95 ± 4.19	89.8 ± 3.84	92.89 ± 3.8
27 weeks after BMT				
BMT	93.9 ± 8.41	78.34 ± 5.8	92.36 ± 6.58	91.28 ± 9.44
BMT + ERT	95.46 ± 3.04	85.48 ± 4.3	94.82 ± 3.05	89.1 ± 4.174

[a] Percentage of donor-derived cells in peripheral blood at 12 or 27 weeks after BMT. The individual values are shown as mean values ± SD (BMT: n = 5, BMT + ERT: n = 5).

Approximately 90% donor cell engraftment in each lineage cell was achieved at 12 and 27 weeks in animals that received BMT alone or in combination with ERT. Percent engraftment of T cell lineage was lower than for other cell lineages probably because of the longer half life time of pre-existing recipient T cells.

3.2. Serum IDS activity in mice treated with BMT, ERT or a combination of BMT and ERT

Serum IDS activities at various time points were assayed following treatment (Fig. 2). MPS II mice treated by BMT alone showed a rise in IDS activity beginning at 2 weeks post-transplantation which reached 25% of WT levels at 20 weeks ($P < 0.001$ vs. untreated MPS II mouse, NT). Animals treated with ERT alone had no detectable serum IDS activity as the infused IDS was rapidly cleared from circulation. Serum IDS levels in mice treated by the combination of BMT and ERT exhibited a profile that was similar to mice treated by BMT alone ($P < 0.001$ vs. NT, $P > 0.05$ vs. BMT). As may be expected the serum IDS enzymatic activity did not increase even after initiation of ERT as the infused enzyme was rapidly cleared from circulation. These observations indicate that the donor cells were stably engrafted in the BMT treated mice and that they excreted IDS for a sustained period.

3.3. Tissue IDS activity in mice treated by BMT or ERT alone and combination of BMT and ERT

Twenty-seven weeks after treatment by BMT or ERT or the combination, IDS activity in various tissues of MPS II mice was analyzed. In the ERT treated group (Fig. 3A), no significant increase in IDS activity

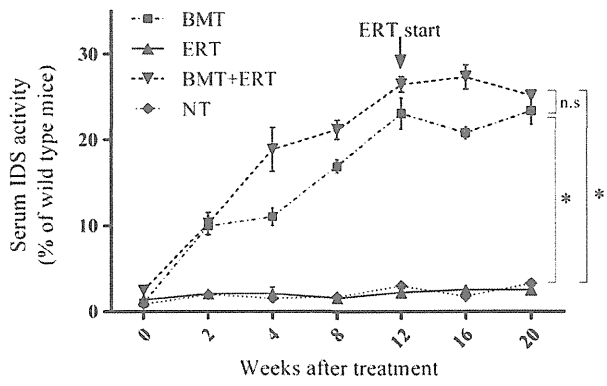

Fig. 2. Sustained IDS activities in serum from BMT received MPS II. IDS activity in serum from MPS II mice in three treatment groups, WT mice and NT mice was measured as described in Methods. The IDS activities were assayed duplicate. Arrows indicate start point of ERT in BMT + ERT group. IDS activity is expressed as % of age matched WT mice (data of WT mice is not shown in figure). The IDS activities at each time point are shown as mean ± SEM (each group: n = 5). The difference of enzyme activities at 20 weeks after treatment was compared by one-way ANOVA among 3 treatment groups and NT group. Asterisk indicates $P < 0.001$. "n.s" indicates no significant difference.

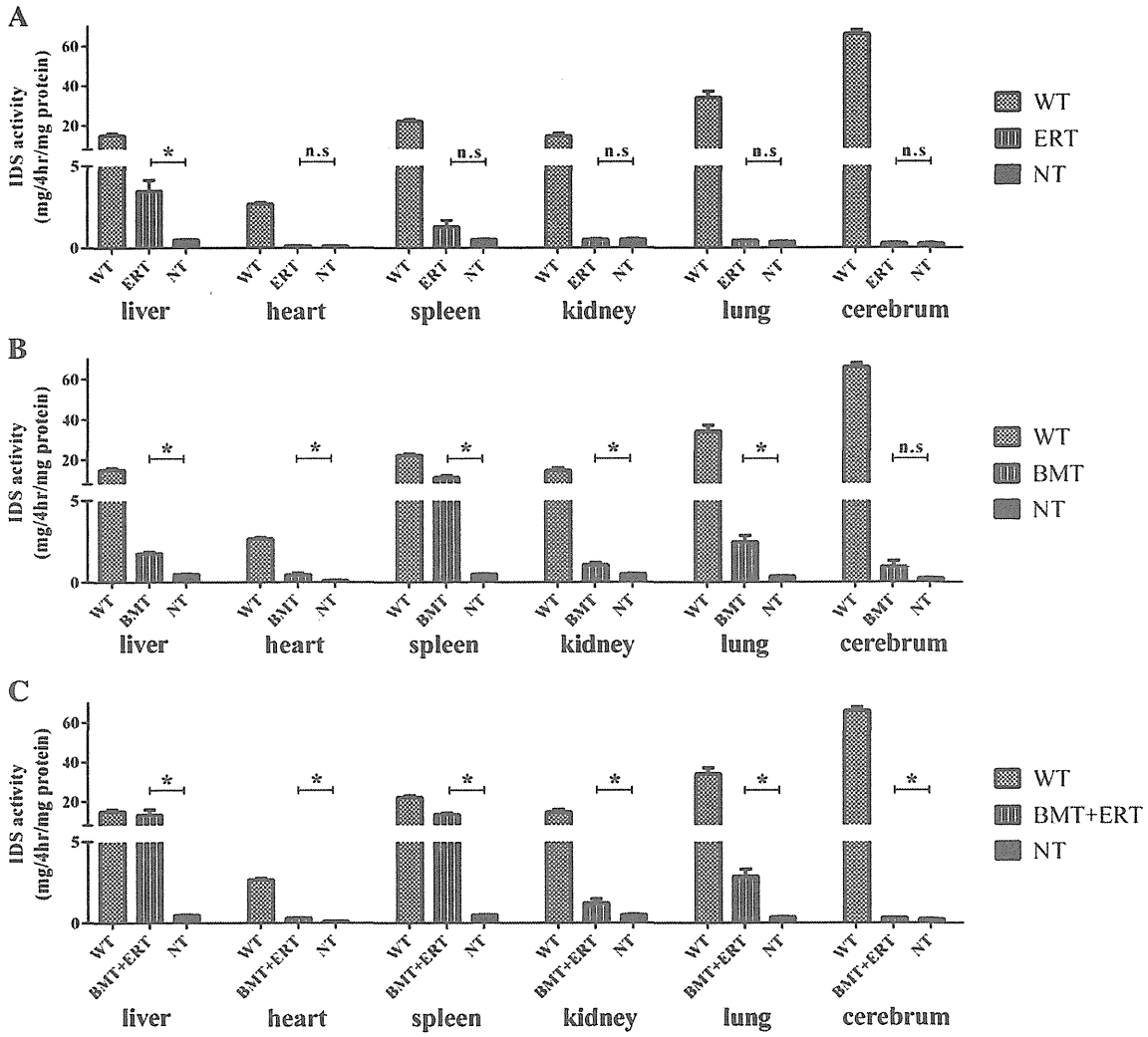

Fig. 3. Increased tissue IDS enzyme activity. Liver, heart, spleen, kidney, lung and cerebrum were harvested from treated mice, age matched WT mice and age matched NT mice at 27 weeks after initiation of treatment. Tissue IDS enzyme activity was measured as described in Methods. IDS activity is expressed as nmol/4 h/mg protein. Data are presented as mean ± SEM (each group: n = 5). Difference of enzyme activity between treatment group and NT group was compared using Student's t-test. Asterisk indicates $P < 0.05$. "n.s" indicates no significant difference.

was observed in any tissues tested, except the liver. As the tissues were harvested one week after the last enzyme infusion, it is likely that the enzyme had already turned over in most of tissues. In the liver, as large amounts of the enzyme were taken up by the cells, we were still able to detect some measure of activity even one week after the last infusion. In the BMT-treated group (Fig. 3B), higher IDS activity was detected in the liver, heart, spleen, kidney and lung but not in cerebrum. Mice treated by a combination of BMT + ERT (Fig. 3C) showed a similar profile of higher IDS activity. Unlike the BMT group, the increase of IDS activity in the cerebrum was statistically significant but the elevation of IDS activity was minimal. These results indicated that stable engraftment of donor cells in recipient mice following BMT led to an increase in IDS activity in various tissues.

3.4. Impact of elevated IDS activity on total tissue GAGs levels

To study the effect of BMT on the CNS disease, the potential for an additive effect of a combination of ERT to BMT and to compare the relative efficacy of BMT and ERT, we analyzed tGAGs levels in various tissues. Analysis of GAGs using the Alcian blue method allows for a determination of tGAGs. In the cerebrum (Fig. 4), none of the treatments reduced tGAGs levels. However, because there was no significant difference in cerebrum tGAGs levels between WT mice and NT MPS II mice, this result is not informative. In liver (Fig. 4, Supplemental Fig. 1), tGAGs were significantly reduced by BMT, ERT and BMT + ERT compared to untreated controls. However, there was no statistical difference among the three treatment groups. There was a suggestion that ERT provided an additive effect to BMT, but this trend was not statistically significant. In the heart and spleen (Fig. 4, Supplemental Fig. 1), all of the treatments reduced tGAGs to almost WT levels. There was no statistical difference among three treatment groups and ERT did not afford additive effect to BMT. In the kidney (Fig. 4, Supplemental Fig. 1), ERT and BMT + ERT significantly reduced tGAGs, but BMT alone did not. ERT reduced tGAG levels more profoundly than BMT and ERT conferred an additive effect to BMT. In the lung (Fig. 4), all treatment regimens reduced tGAGs significantly. ERT reduced tGAGs more profoundly than BMT and ERT conferred an additive effect to BMT. Hence, an additive effect of ERT to BMT was observed in the kidney and lung, and ERT was superior to BMT at reducing tGAGs in the kidney and lung.